NASA/TM-20250003541



Acoustics Testing of Second-Generation Pratt & Whitney Geared Turbofan Model in NASA Glenn 9- by 15-Foot Low-Speed Wind Tunnel

David M. Elliott
Glenn Research Center, Cleveland, Ohio

June 2025

NASA STI Program Report Series

Since its founding, NASA has been dedicated to the advancement of aeronautics and space science. The NASA scientific and technical information (STI) program plays a key part in helping NASA maintain this important role.

The NASA STI program operates under the auspices of the Agency Chief Information Officer. It collects, organizes, provides for archiving, and disseminates NASA's STI. The NASA STI program provides access to the NTRS Registered and its public interface, the NASA Technical Reports Server, thus providing one of the largest collections of aeronautical and space science STI in the world. Results are published in both non-NASA channels and by NASA in the NASA STI Report Series, which includes the following report types:

- TECHNICAL PUBLICATION.
  Reports of completed research or a major significant phase of research that present the results of NASA programs and include extensive data or theoretical analysis. Includes compilations of significant scientific and technical data and information deemed to be of continuing reference value. NASA counterpart of peer-reviewed formal professional papers but has less stringent limitations on manuscript length and extent of graphic presentations.

- TECHNICAL MEMORANDUM.
  Scientific and technical findings that are preliminary or of specialized interest, e.g., quick release reports, working papers, and bibliographies that contain minimal annotation. Does not contain extensive analysis.

- CONTRACTOR REPORT.
  Scientific and technical findings by NASA-sponsored contractors and grantees.

- CONFERENCE PUBLICATION.
  Collected papers from scientific and technical conferences, symposia, seminars, or other meetings sponsored or cosponsored by NASA.

- SPECIAL PUBLICATION.
  Scientific, technical, or historical information from NASA programs, projects, and missions, often concerned with subjects having substantial public interest.

- TECHNICAL TRANSLATION.
  English-language translations of foreign scientific and technical material pertinent to NASA's mission.

Specialized services also include organizing and publishing research results, distributing specialized research announcements and feeds, providing information desk and personal search support, and enabling data exchange services.

For more information about the NASA STI program, see the following:

- Access the NASA STI program home page at http://www.sti.nasa.gov

NASA/TM-20250003541



Acoustics Testing of Second-Generation Pratt & Whitney Geared Turbofan Model in NASA Glenn 9- by 15-Foot Low-Speed Wind Tunnel

David M. Elliott
Glenn Research Center, Cleveland, Ohio

National Aeronautics and
Space Administration

Glenn Research Center
Cleveland, Ohio 44135

June 2025

This work was sponsored by the Advanced Air Vehicles Program
at the NASA Glenn Research Center.

Trade names and trademarks are used in this report for identification only. Their usage does not constitute an official endorsement, either expressed or implied, by the National Aeronautics and Space Administration.

Level of Review: This material has been technically reviewed by technical management.

This report is available in electronic form at https://www.sti.nasa.gov/ and https://ntrs.nasa.gov/

NASA STI Program/Mail Stop 050
NASA Langley Research Center
Hampton, VA 23681-2199

Acoustics Testing of Second-Generation Pratt & Whitney Geared Turbofan Model in NASA Glenn 9- by 15-Foot Low-Speed Wind Tunnel

David M. Elliott
National Aeronautics and Space Administration
Glenn Research Center
Cleveland, Ohio 44135

Summary

A second-generation Pratt & Whitney geared turbofan model was tested in the NASA Glenn Research Center 9- by 15-Foot Low-Speed Wind Tunnel. The main objectives of the test were to determine noise signatures of two inlets and two nozzles. Acoustic variation with angle of attack was investigated along with a full fan tip speed range sweep. Additional microphone measurements were also obtained to get more azimuthal variation of the radiated noise pattern of the model.

Introduction

Pratt & Whitney has been investigating the benefits of using a gearbox to optimize the efficiency of the gas turbine engine. The gear box is used to operate both the fan and the low-pressure spool at their respective optimal speeds to improve the core efficiency. A second-generation model of a geared turbofan (GTF) was tested in the NASA Glenn Research Center 9- by 15-Foot Low-Speed Wind Tunnel (9×15 LSWT) to investigate the acoustic performance of the model with two inlets and two nozzles. Angle-of-attack (AOA) measurements were also taken to characterize the AOA effect on noise. Lastly, some additional measurements were made to determine the azimuthal variation of the noise pattern.

Test Hardware

The NASA Glenn Universal Propulsion Simulator (UPS) was used as the drive system for the Pratt & Whitney GTF model. Turbines within the drive rig are fed by a 450-psi air source, which turns the fan. The UPS is fixed on a turntable, enabling the rotation of the entire drive rig to simulate AOA in the tunnel. The model hardware consisted of the fan, bypass outlet guide vanes, and core inlet guide vanes, as well as the inlet, nacelle, nozzle, and core inlet. The model has 14 fan blades, 24 bypass outlet guide vanes, and 16 core inlet guide vanes. The fan blades are representative of latest-generation GTF designs. Two inlets were tested; one had a short inlet designed to reduce skin friction drag and the other was a conventional inlet that includes droop at the 0° circumferential point (top dead center). Two nozzles were also tested: one designed for cruise condition (called the sideline nozzle) and the other designed for approach condition (approach nozzle). The data from the two nozzles provide some guidance on the utility of a variable area nozzle in real-world conditions.

Test Matrix

There were four main configurations for this test, which included four combinations of two inlets and two nozzles. These configurations were tested at different AOA settings ranging from –10° to +20° or a

subset thereof. Although some data was obtained at the wind tunnel free-stream speed of Mach 0.1 for comparison to historical tests, the data presented here was obtained at Mach 0.2. Tests at the Mach 0.2 speed were necessary to simulate the correct operating conditions for a short inlet. The corrected fan tip speeds (designated as "rpmc") tested ranged from 5,000 to 10,500 rpmc or a subset of this range.

Test Facility

This test was conducted in the NASA Glenn Research Center 9×15 LSWT (Refs. 1 to 3). The 9×15 LSWT has acoustically treated walls using Kevlar® batting (DuPont Safety & Construction, Inc.) batting. The maximum flow velocity is approximately 0.22 to 0.23 Mach.

Sideline Acoustics

Sideline acoustic measurements were obtained using a traversing microphone probe on a track parallel to the fan axis at a distance of 89 in. Data were taken at 48 positions on the traverse at 2.5° intervals ranging from 27° to 135° relative to the fan stacking axis, with 0° at the upstream infinity. The traversing probe is a new design incorporating three microphones instead of one, as in the original traversing probe. This allows for obtaining two additional azimuthal measurements at each axial station. All three microphones are at the same radial distance from the model centerline (i.e., 89 in.). At a freestream Mach number of 0.2, the emitted angle range of the traversing microphone is from 22° to 126°.

Three fixed microphones are also typically placed on the floor of the test section between the traversing microphone and the fan model. These microphones provide additional angular measurements of 140°, 150°, and 160°. The corresponding emitted angles at a freestream Mach number of 0.2 for the fixed floor microphones are 133°, 144°, and 156°, respectively. Two additional microphones were placed upstream of the model on the ceiling and floor of the test section. These microphones were located in the same axial plane as the traversing microphone when it is at approximately the 60° position on the traverse track. These two microphones were also used to measure azimuthal variation of the inlet noise of the model. All microphones were 1/4 in. in diameter and included nose cones for in-flow measurements. The nose cones used in this test are based on the Flow Induced Tone Eliminator (FITE) design developed at the NASA Ames Research Center.

Data were taken at a sampling rate of 200 kHz to ensure a Nyquist frequency upper limit of at least 60 kHz. This would permit scaling this data to full-scale for system analysis purposes. Corrections to the data have been made for microphone response, bullet nose receptivity, atmospheric attenuation, and spherical spreading. All far-field data shown are lossless, projected onto a 1-ft arc centered on the fan origin located at the intersection of the rotor plane with the rotor rotational axis. The accuracy of the data system is ±1 dB in sound pressure level (SPL) (Ref. 4). The test section containing the model and microphones in the acoustic configuration is shown in Figure 1. Note that the traversing microphone starts in the aft position and moves upstream during the test.

Results

Inlet and Nozzle Comparisons

Figure 2 and Figure 3 show overall power levels versus corrected fan tip speed for different inlet and nozzle combinations. The power levels were calculated using the SPL data from the 48 traverse microphone stops, as well as the three floor microphones. The frequency range for the calculations was restricted to 1 to 50 kHz. The lower limit ensures that no contribution from extraneous sources such as the

bypass jet are included in the fan noise calculations. The upper limit represents the highest model-scale frequency that would be matched to a full-scale rating frequency of 10 kHz. For the large majority of speed conditions, the short inlet had lower levels than the conventional inlet with either nozzle, although the difference was slightly greater for the approach nozzle. The only condition at which the short inlet had higher levels than the conventional inlet was at the highest speed for the sideline nozzle. The short and conventional inlets showed similar levels for the sideline nozzle in the 9,000- to 10,000-rpmc range. In general, the differences were not greater than 1 dB. It is also interesting to note that, regardless of the inlet used, the shape of the spectrum was similar for the same nozzle. The sideline nozzle also had lower levels when used with either inlet compared with the approach nozzle. Once again, the differences are small, no more than 3 dB and usually less.

Figure 4 to Figure 6 show some example spectra for the short and conventional inlets using the sideline nozzle. All the spectra in this report have been reduced to 1-ft lossless by correcting for the atmospheric attenuation over the radiation distance. For most of the spectra shown in this report, there is an abundance of tonal energy. In general, focusing on the broadband noise differences will explain the power level results. In the 5,000-rpmc case shown in Figure 4, the higher broadband levels at and lower than 20 kHz for the conventional inlet are evident at the three emission angles shown. In Figure 5, which shows the 8,000-rpmc case, the broadband differences are greater in the inlet quadrant than in the broadside and aft quadrant. In the 10,500-rpmc case shown in Figure 6, the broadband levels for the conventional inlet are slightly higher in the upper frequency range of 30 kHz and higher.

Figure 7 to Figure 9 show example spectra for three speeds for the short and conventional inlets with the approach nozzle. In most of these cases, the broadband levels are not that different, the exceptions being the 6,153-rpmc case at 22° emitted angle, where the high-frequency noise is actually higher for the short inlet, and for the lower frequency ranges of the 10,500-rpmc case at 22°, where the short inlet now is quieter. It does appear that this is one case in which additional tonal energy is present in the conventional inlet configuration, resulting in the higher power levels. This can be seen in the 126° emitted angles of the 6,153-rpmc case of Figure 7 and the 8-000-rpmc case of Figure 8.

The spectra shown in Figure 10 to Figure 12 again show a higher broadband level, this time for the approach nozzle relative to the sideline nozzle when used with the short inlet. The broadband levels for the conventional inlet are particularly elevated at higher frequencies for the 6,153-rpmc case of Figure 10 and the 9,484-rpmc case of Figure 12.

For the sideline and approach nozzle comparisons used with the conventional inlet, Figure 13 shows that at 6,153 rpmc there appears to be a hump in the 3 to 10 kHz range in which the sideline nozzle has a higher noise level, particularly at 22° and 84° emitted angles. At higher frequencies, the nozzle configurations are similar at 84° and the sideline nozzle has a lower level at 22° and 126°. The approach nozzle produces more tonal energy at this speed. At 8,000 rpmc, Figure 14 shows that the broadband level of the sideline nozzle is somewhat higher at 22°, but the trend reverses and the sideline nozzle becomes quieter at 84° and at 126°. Figure 15 shows mostly higher broadband levels for the approach nozzle except in the higher frequencies at the 22° emitted angle. It should also be noted that there is a large increase in tonal energy for all configurations at the 9,484- and 10,500-rpmc cases, particularly in the higher emitted angle regions. This is particularly obvious in Figure 15 at 126°, where the approach nozzle tones are quite noticeable. Another note of interest is that broadband levels are not that different between the inlet and aft quadrants. This is in contrast to past high-bypass-ratio model data, in which the aft fan noise levels were usually highly dominant.

Angle-of-Attack Results

Figure 16 shows power level versus corrected fan tip speed for four different AOA for the short inlet and sideline nozzle configuration and two different AOA for the conventional inlet and sideline nozzle configuration. When the AOA is increased positively, simulating takeoff engine orientation, the noise levels increase due to the inlet flow being distorted. This is mostly true in the mid-speed range, where the levels change on the order of 1 dB per 10° change in AOA. However, at the lower speeds and, interestingly, at higher speeds, the differences are not as great. It has been speculated that this could be due to a high level of turbulence at lower speeds regardless of AOA and a lower level of flow turbulence at higher speeds due to the higher momentum from the increased inlet velocity. In any case, power levels that are within ±1 dB of each other are effectively the same.

Of particular interest is the –10° AOA for the short inlet sideline nozzle configuration, which shows similar levels as the 0° AOA until about 9,000 rpmc, after which the level increases to magnitudes higher than 10° AOA by as much as 4 dB. For the lower speeds, even though an in-flow disturbance would be predicted, some other phenomena are taking place. The higher speeds could be indicative of a larger in-flow disturbance for the inlet as opposed to positive AOA. Figure 17 shows spectral comparisons of the short inlet sideline nozzle at 0° and 10° AOA for 5,000 rpmc. Here, it can be seen that as the measurements increase from forward angles to aft angles, the broadband for 10° AOA increases. The appearance of additional tones also occurs from forward to aft measurements. Figure 18 shows spectra for the short inlet sideline nozzle for 0° and 20° AOA at 6,153 rpmc. Interestingly, the broadband levels for 20° are lower for the 22° emitted angle, possibly due to the fact that the inlet is now pointing away from the microphones. For the 84° and 126° measurement locations, the broadband and tones increase for the 20° AOA as expected. Figure 19 shows spectra of the short inlet sideline model at 8,000 rpmc for the four AOA of 0°, 10°, 20°, and –10°. Although the different AOA have the same noise characteristics at 22°, the pattern at 88° and 126° mimics the power level results, with rising broadband levels going from –10° to +20° AOA. Figure 20 shows the short inlet sideline nozzle spectra for 0° and 20° AOA at 9,484 rpmc; Figure 21 shows the spectra for 0° and 10° AOA at 10,500 rpmc. Both Figure 20 and Figure 21 show the same characteristics, higher broadband for the larger AOA, especially as the measurements progress from low emitted angles to large emitted angles.

Figure 22 to Figure 24 show spectra for the conventional inlet sideline nozzle for 0° and 10° AOA for the three shaft speeds of 5,000, 8,000, and 10,500 rpmc. At 5,000 rpmc, there is little difference between 0° and 10° AOA for the 22° emitted angle, with the 10° AOA becoming slightly greater at higher frequencies for the 84° and 126° emitted angles. At 22°, the 8,000-rpmc condition shows a low-frequency broadband hump for the 0° AOA relative to the 10° AOA, but at higher frequencies the situation changes with the 10° AOA having a higher level. This situation holds for the higher emitted angles of 84° and 126° AOA. Lastly, at 10,500 rpmc, once again there is little difference at 22° emitted angle and the 10° AOA becomes greater at higher frequencies for 84° and 126° emitted angles.

Azimuthal Variation

The short inlet and the droop conventional inlet (which is nonaxisymmetric) sparked an interest in obtaining more azimuthal measurements than normally taken in typical fan tests in the 9×15 LSWT. The two additional microphones on the traversing probe and ceiling and floor microphones upstream of the model, described previously in the Sideline Acoustics section, were deployed for this purpose. Figure 25 shows spectra for the short inlet with the sideline nozzle at 5,000 rpmc. The axial plane containing the 60°

geometric angle also contains the upstream ceiling and floor microphones. The 60° geometric angle corresponds to a 49° emitted angle at Mach 0.2. The top and bottom microphones on the traversing probe have azimuthal angles of +22.5° and –22.5° with the center microphone located at 0° azimuth. The top and bottom microphones are referred to as "+22.5° AZ" and "–22.5° AZ," respectively, in Figure 25 to Figure 30.

For the three traversing probe microphones, the top and middle locations show similar levels at 49° and 126° emitted angles. The bottom floor microphone has a higher level for both emitted angles. This result is also seen in Figure 26 and Figure 27 for the 8,000- and 10,500-rpmc speeds. This could be due to the way that the bottom microphone is mounted, cantilevered out behind the airfoil that contains the top and middle microphones. The bottom microphone is also closer to the traversing drive mechanism and may be picking up some airflow noise over this mechanism. For the three speeds at 49°, the ceiling microphone shows lower levels than the traversing probe microphones, and the floor microphone shows even lower levels than the ceiling microphone. This may indicate that for the short inlet there exists an azimuthal pattern that has lower levels at the 90° and 270° positions relative to the droop incorporated in the conventional inlet. Figure 28 to Figure 30 show the spectra for the same azimuthal positions for the conventional inlet with sideline nozzle. Similar results are seen for the three microphones on the traverse, that is, higher levels for the bottom microphone; however, there are some exceptions in this case. The middle traversing microphone shows higher low-frequency broadband levels than the top and bottom microphones at 5,000 rpmc and 49° emitted angle than at 8,000 rpmc. The top microphone broadband levels follow the bottom microphone levels at the 10,500-rpmc speed and 126° emitted angle. At the 49° emitted angle, once again the ceiling and floor microphones show lower broadband levels than the traversing microphones, the difference this time being that the floor and ceiling levels are very similar.

Conclusions

A scale model test of a second-generation Pratt & Whitney geared turbofan model rig in the NASA Glenn Research Center 9- by 15-Foot Low-Speed Wind Tunnel shows lower noise levels for a short inlet compared with a conventional droop inlet regardless of whether a sideline or approach nozzle was used. The sideline nozzle shows lower noise levels compared to the approach nozzle regardless of which inlet was used. Aside from a few exceptions, the quieter configurations show lower broadband noise levels, especially at higher frequencies. There are also a few instances for which the quieter configurations have less tonal energy at the lower frequencies. Noise levels also increase as the angle of attack changes from –10° to +20°. This increase is greater at the mid-speed range and less for the lower- and upper-speed ranges. As in the inlet and nozzle data comparisons, the angle of attack spectra suggest that most level variations are due to increases in broadband levels and occasionally due to the changes in the levels of tones. Finally, measurements taken by the top and bottom microphones on the traversing probe and by the upstream ceiling and floor microphones provide some sense of the azimuthal variations of the noise field. These measurements show a higher level from the bottom traversing microphone compared to the top and middle positions. The upstream ceiling and floor microphones show lower levels relative to the traversing probe microphones, indicating a lower noise signature at the 90° and 270° positions relative to top dead center of the inlet.

References

1. Dahl, Milo D.; and Woodward, Richard P.: Comparison Between Design and Installed Acoustic Characteristics of NASA Lewis 9- by 15-Foot Low-Speed Wind Tunnel Acoustic Treatment. NASA TP–2996, 1990. https://ntrs.nasa.gov
2. Dahl, Milo D.; and Woodward, Richard P.: Acoustical Evaluation of the NASA Lewis 9- by 15-Foot Low Speed Wind Tunnel. NASA TP–3274, 1992. https://ntrs.nasa.gov
3. Woodward, Richard P., et al.: Background Noise Levels Measured in the NASA Lewis 9- by 15-Foot Low-Speed Wind Tunnel. NASA TM–106817 (AIAA 95–0720), 1995. https://ntrs.nasa.gov
4. Dahl, Milo D., ed.: Assessment of NASA's Aircraft Noise Prediction Capability. NASA/TP—2012-215653, 2012, pp. 123–124. https://ntrs.nasa.gov



Figure 1.—Acoustic configuration of 2013 Pratt & Whitney GTF model in NASA Glenn Research Center 9- by 15-Foot Low-Speed Wind Tunnel (9×15 LSWT).

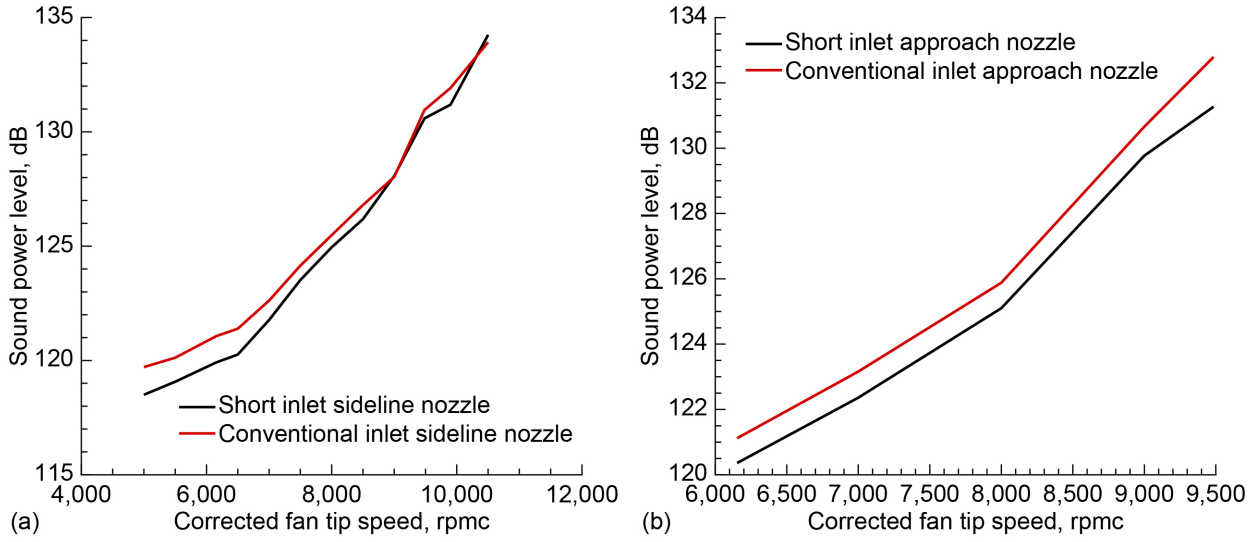

Figure 2.—Overall power levels versus corrected speed (rpmc), comparing short and conventional inlets. (a) For sideline nozzle. (b) For approach nozzle.

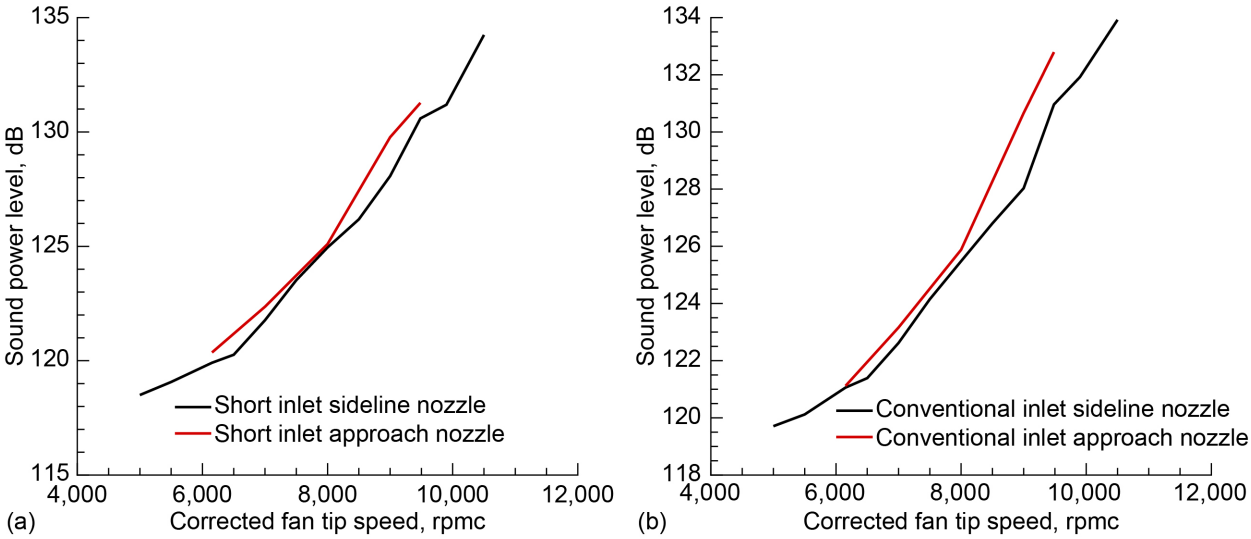

Figure 3.—Overall power levels versus corrected rpm, comparing the sideline and approach nozzles. (a) For short inlet. (b) For conventional inlet.

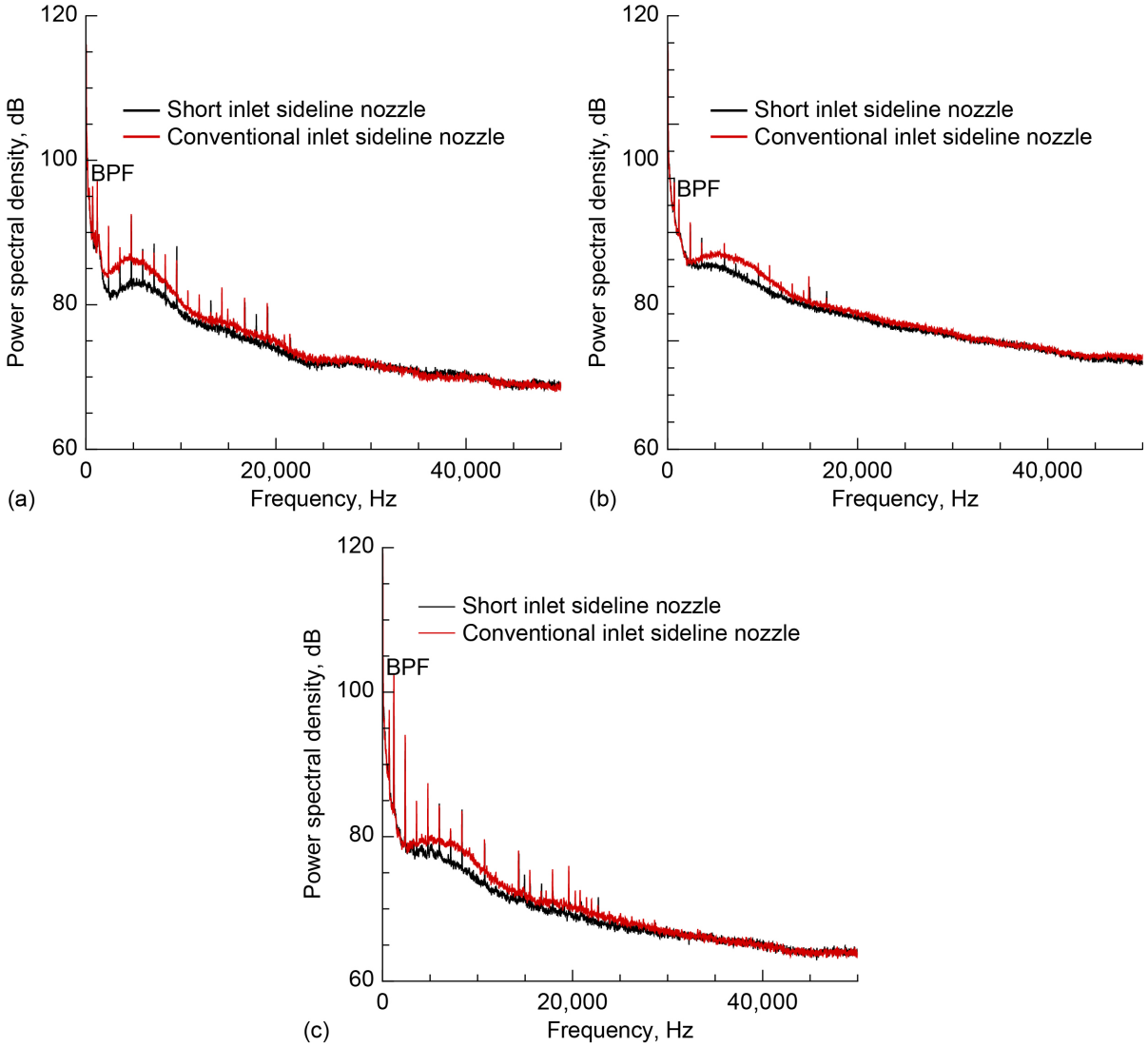

Figure 4.—One-foot lossless spectra for 5,000-rpmc condition, showing short and conventional inlet comparisons using sideline nozzles. (a) At 22°. (b) At 84°. (c) At 126°.[1]

[1]BPF=blade passing frequency

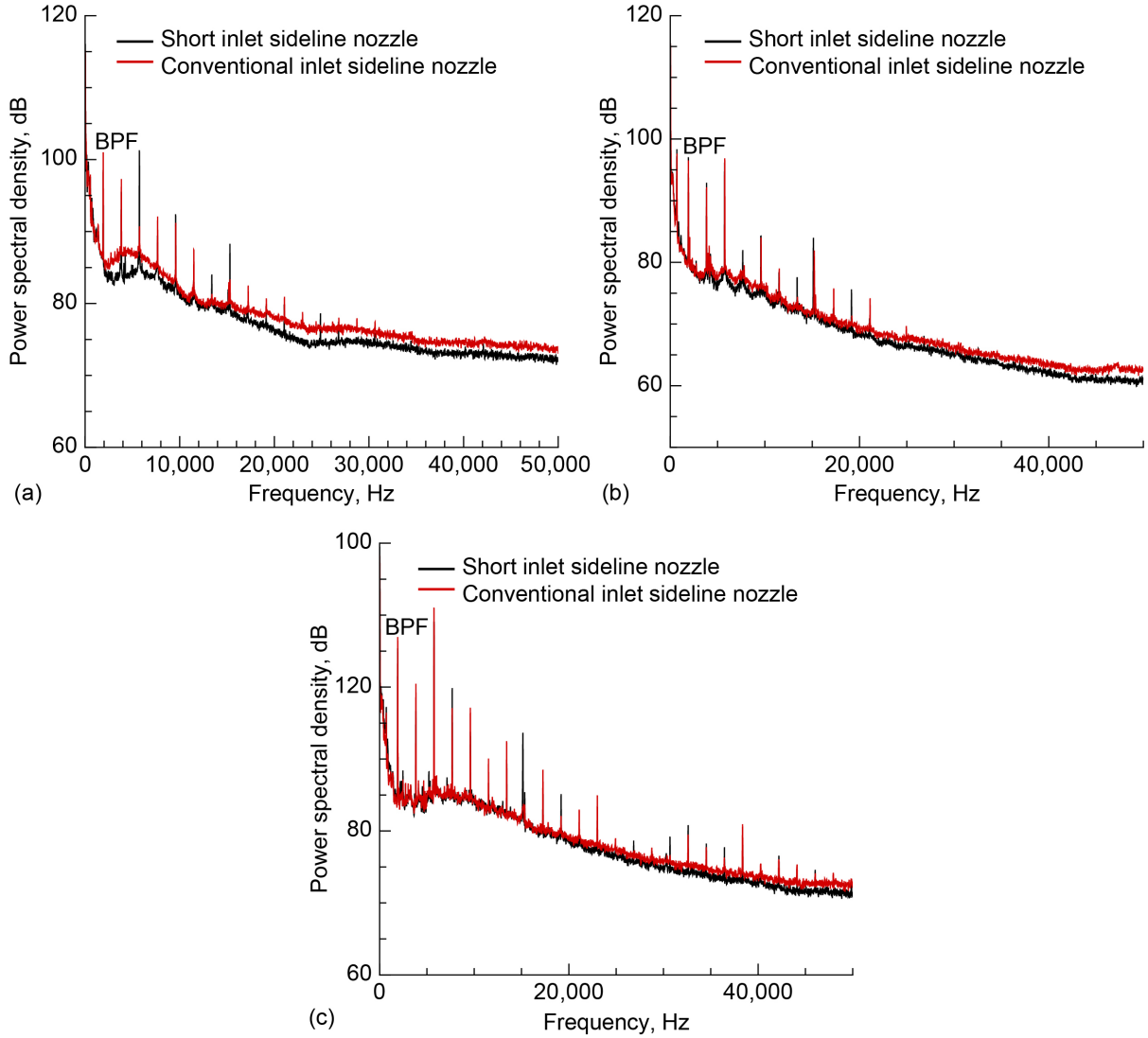

Figure 5.—One-foot lossless spectra for 8,000-rpmc condition, showing short and conventional inlet comparisons using sideline nozzles. (a) At 22°. (b) At 84°. (c) At 126°.

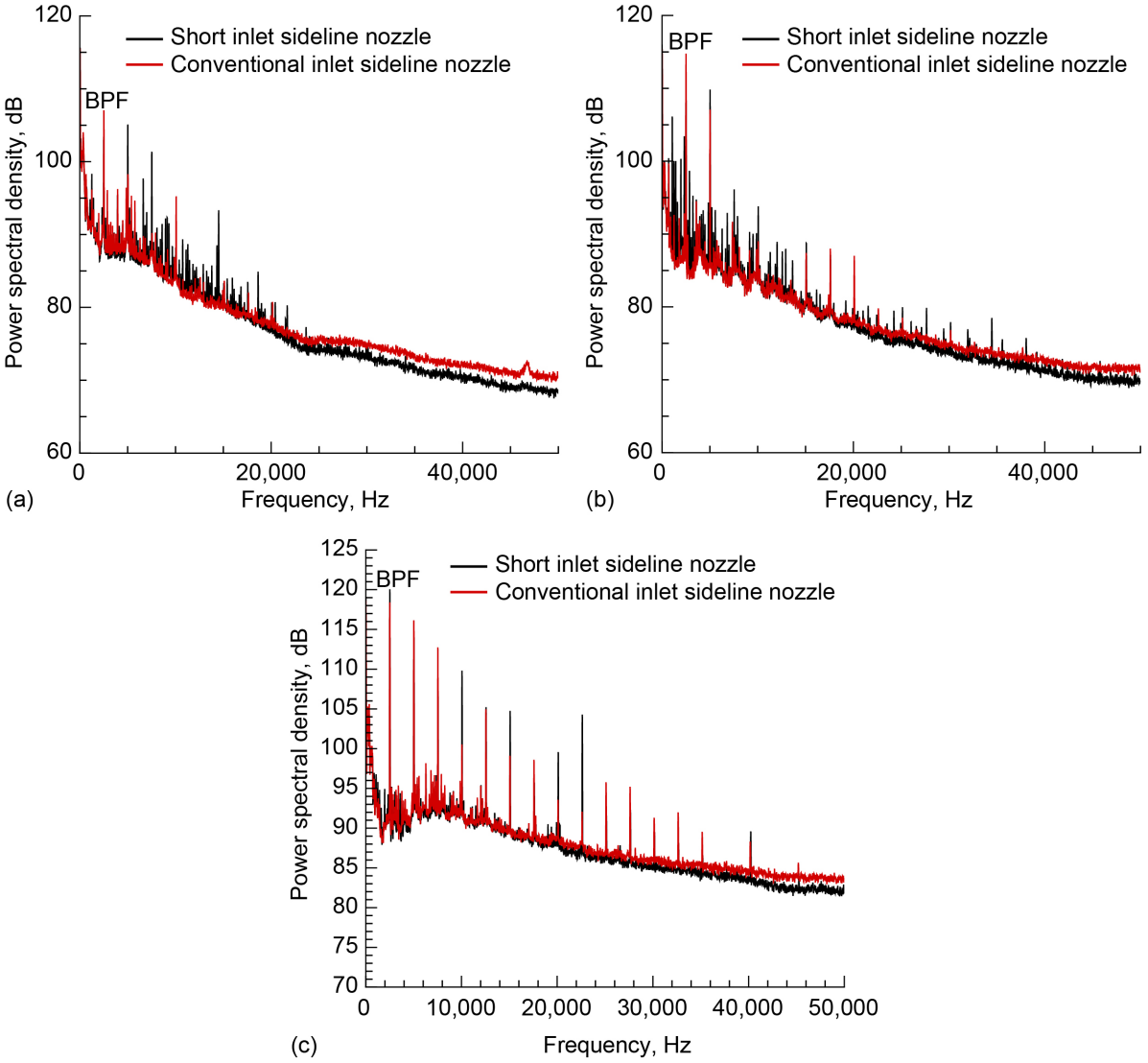

Figure 6.—One-foot lossless spectra for 10,500-rpmc condition, showing short and conventional inlet comparisons using sideline nozzles. (a) At 22°. (b) At 84°. (c) At 126°.

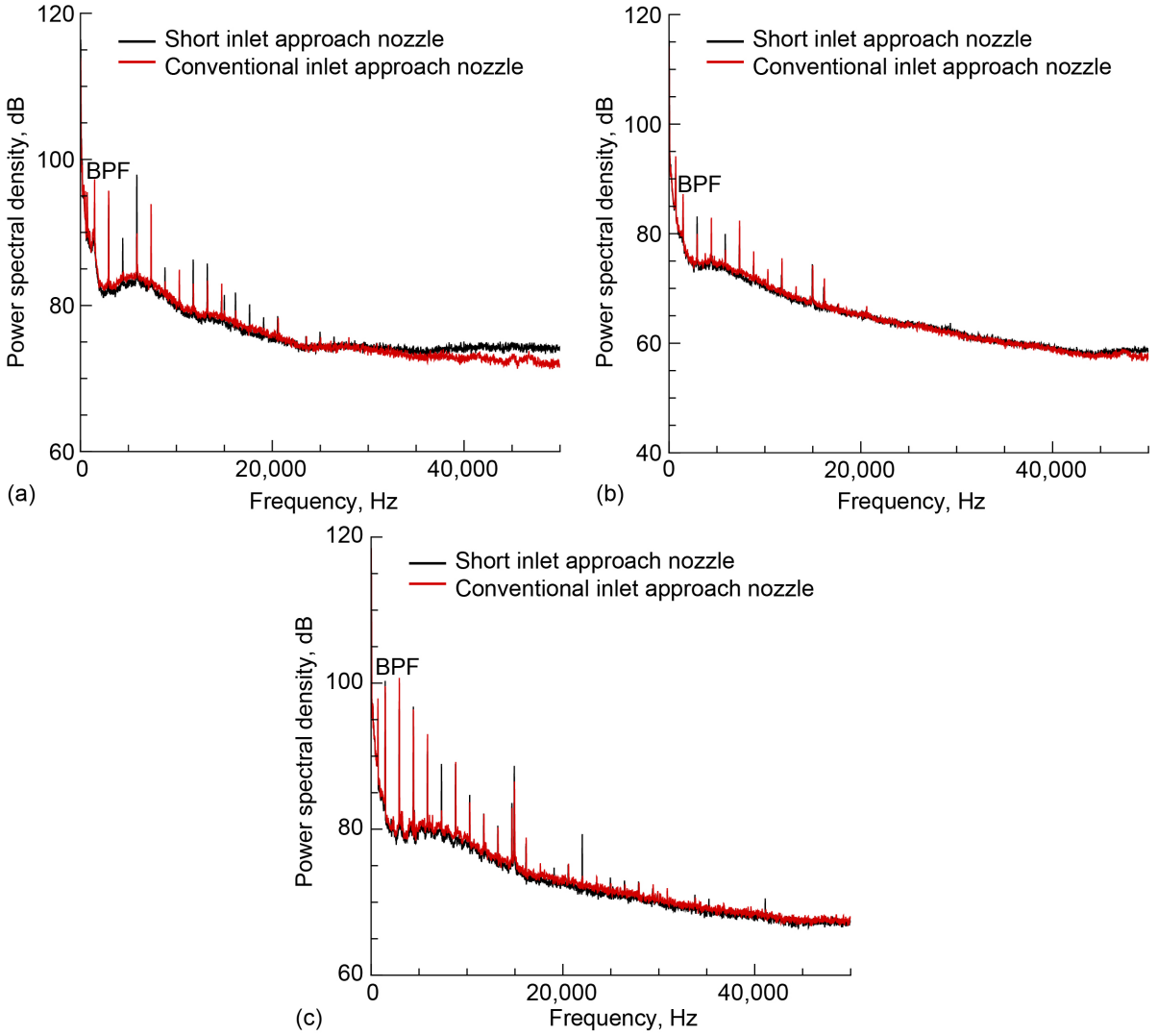

Figure 7.—One-foot lossless spectra for 6,153-rpmc condition, showing short and conventional inlet comparisons using approach nozzle. (a) At 22°. (b) At 84°. (c) At 126°.

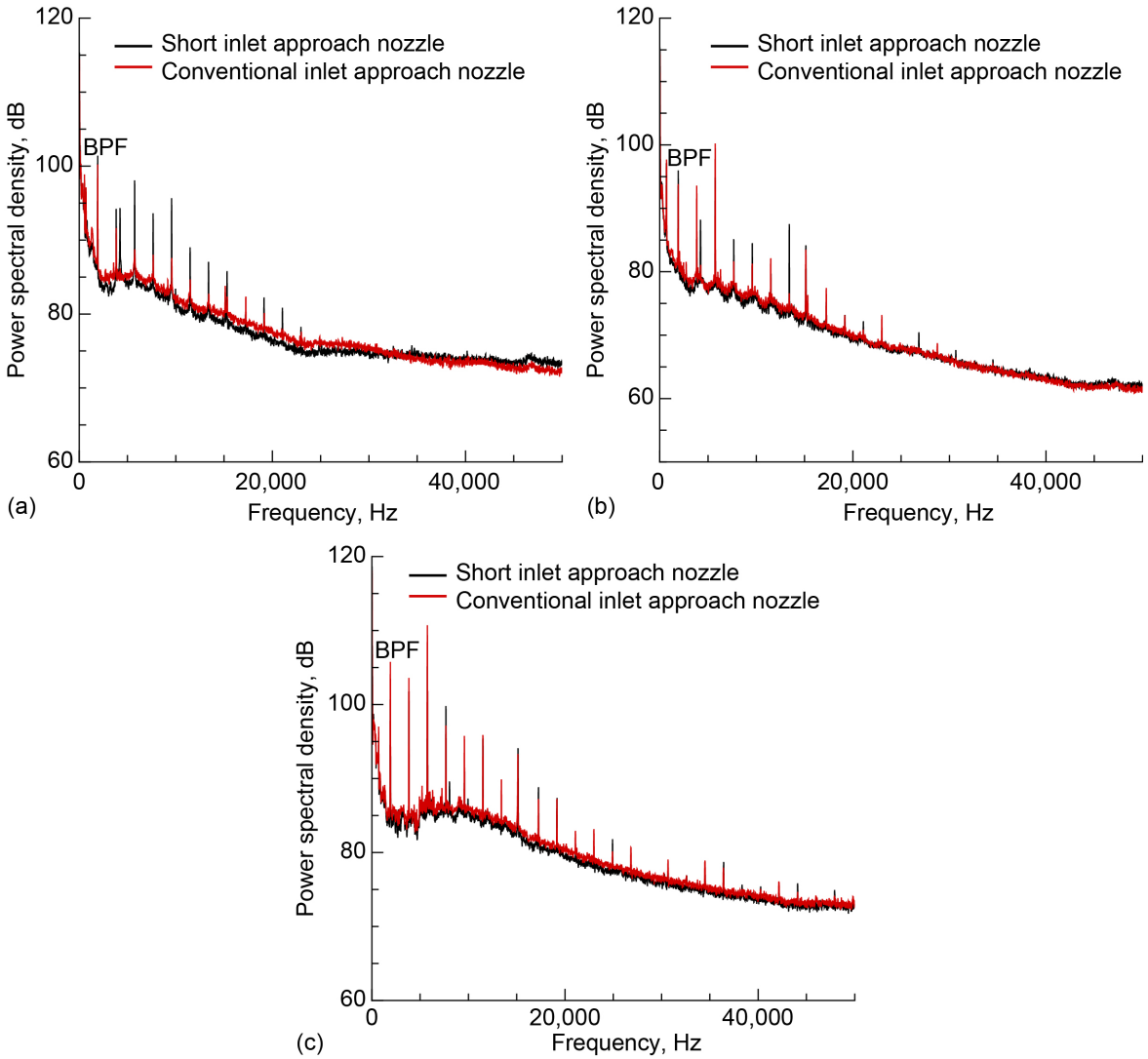

Figure 8.—One-foot lossless spectra for 8,000-rpmc condition showing short and conventional inlet comparisons using approach nozzle. (a) At 22°. (b) At 84°. (c) At 126°.

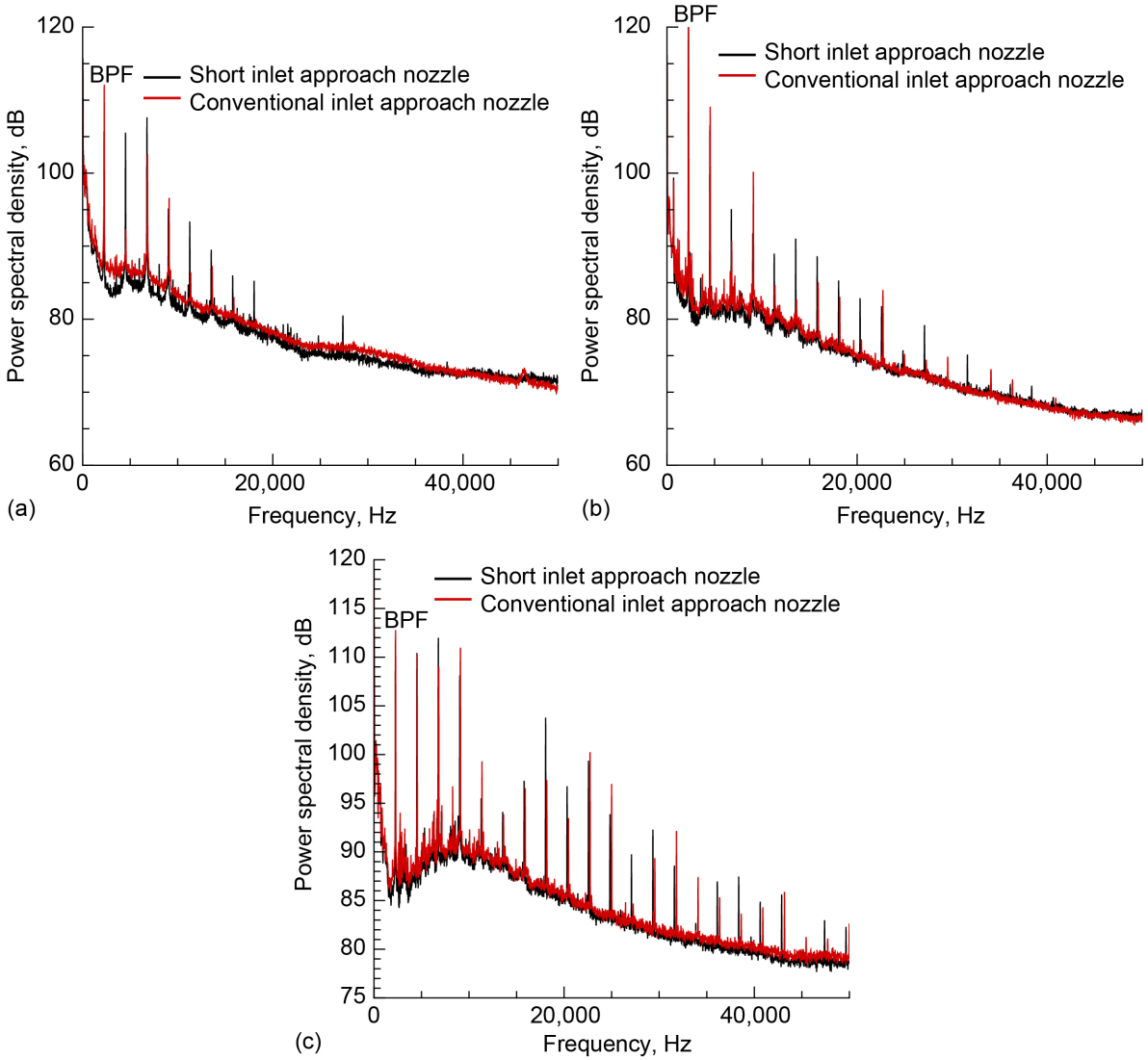

Figure 9.—One-foot lossless spectra for 10,500-rpmc condition, showing short and conventional inlet comparisons using approach nozzle. (a) At 22°. (b) At 84°. (c) At 126° .

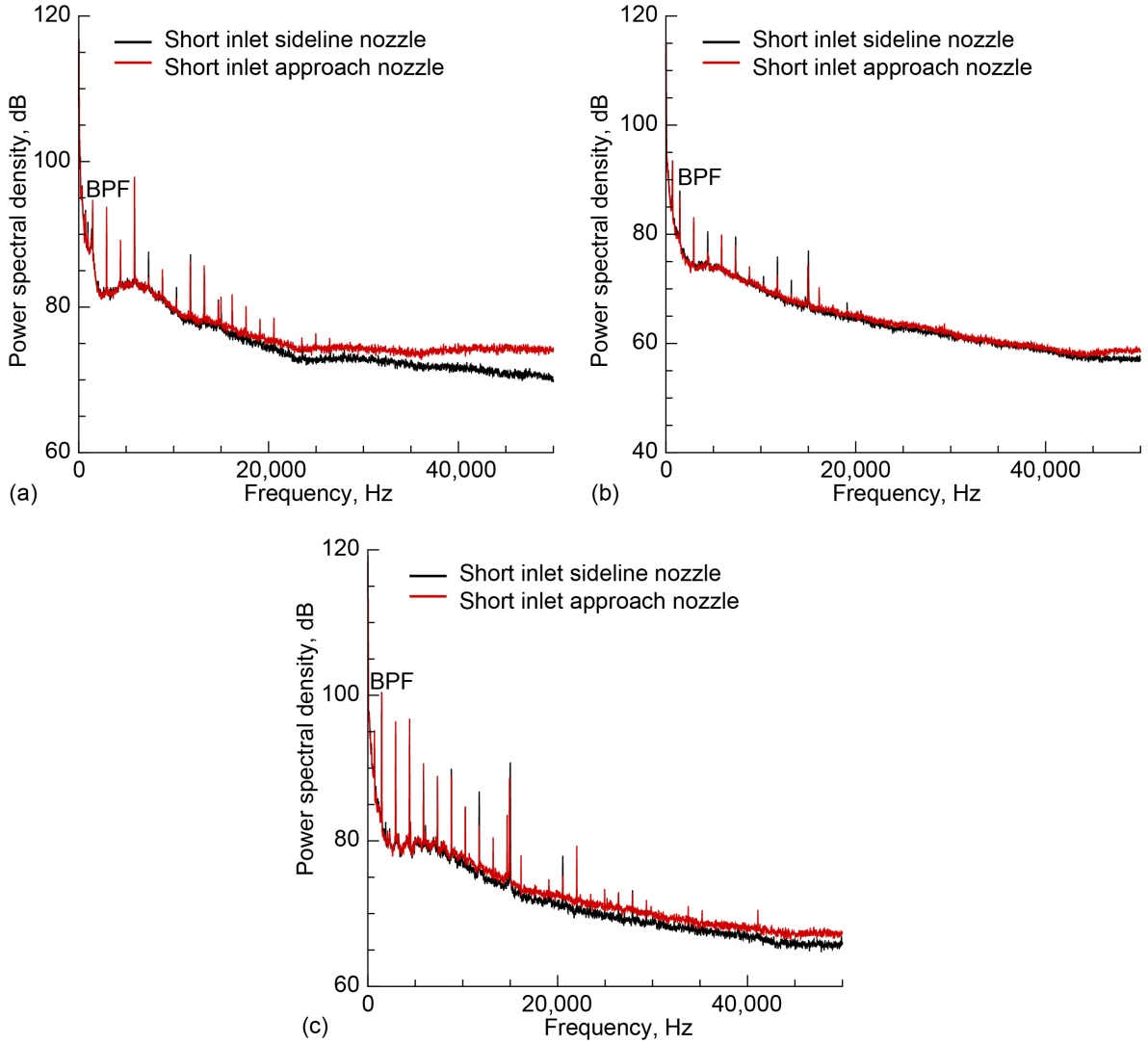

Figure 10.—One-foot lossless spectra for 6,153-rpmc condition, showing sideline and approach nozzle comparisons using short inlet. (a) At 22°. (b) At 84°. (c) At 126°.

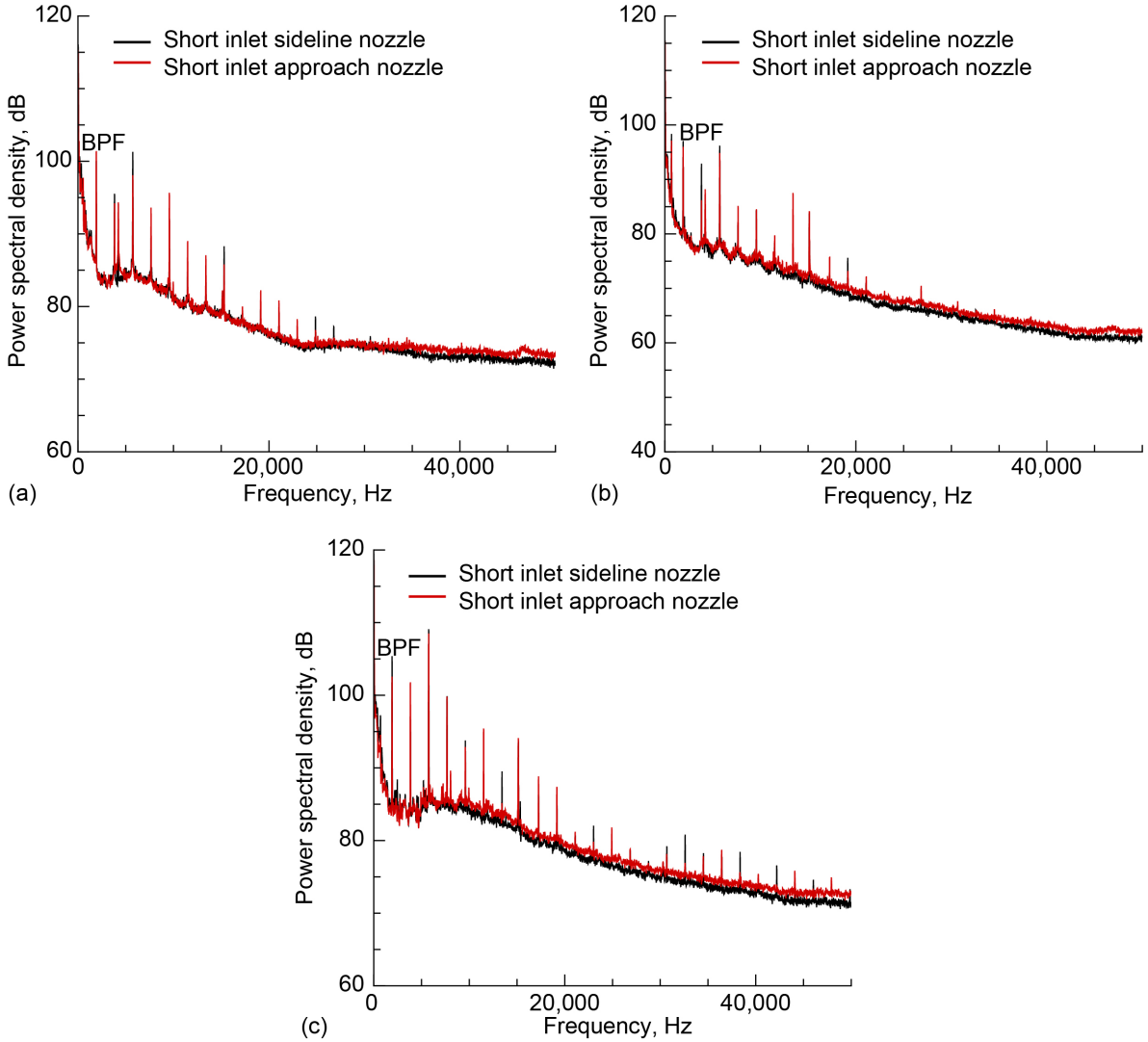

Figure 11.—One-foot lossless spectra for 8,000-rpmc condition, showing sideline and approach nozzle comparisons using short inlet. (a) At 22°. (b) At 84°. (c) At 126°.

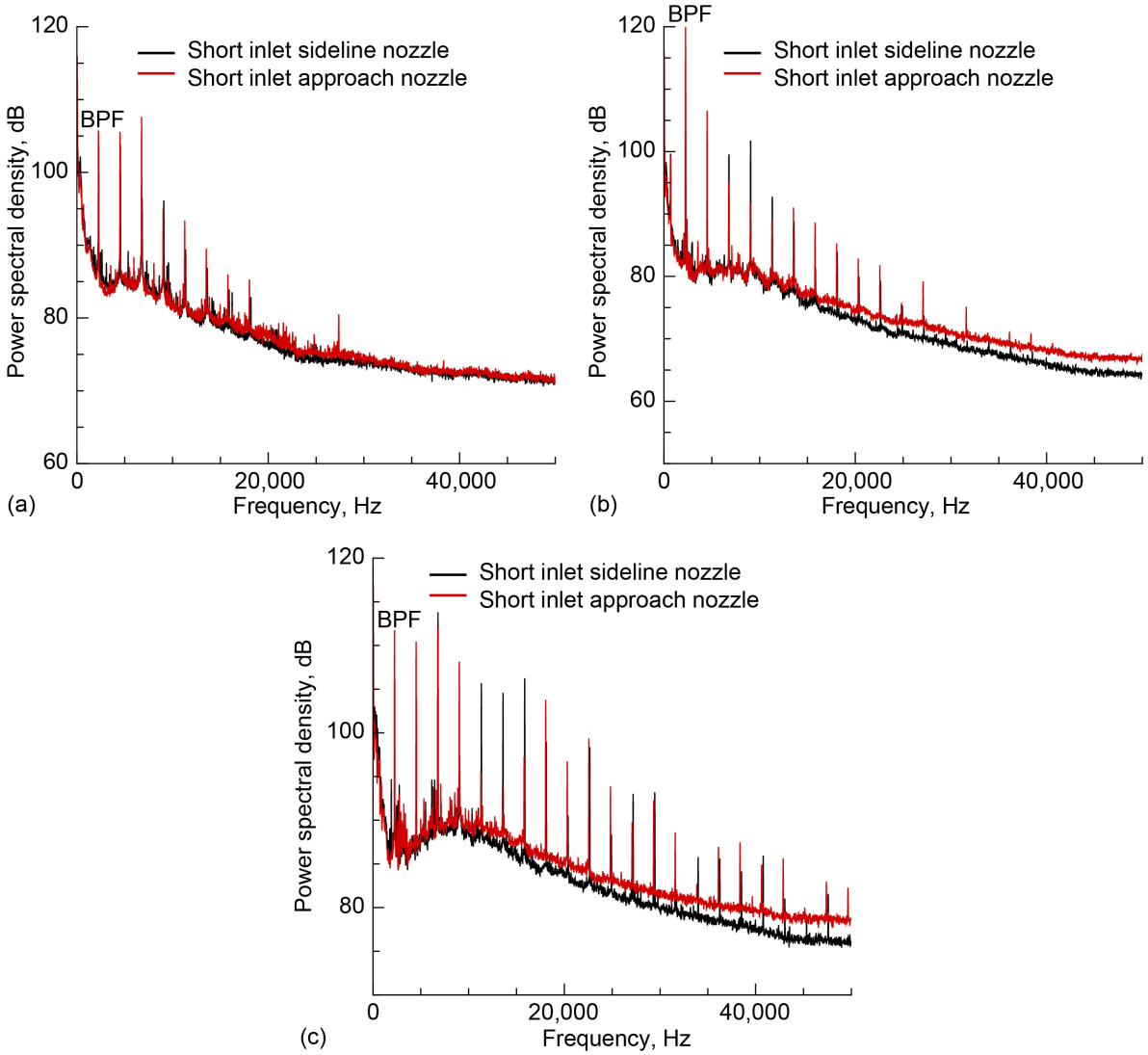

Figure 12.—One-foot lossless spectra for 9,484-rpmc condition, showing sideline and approach nozzle comparisons using short inlet. (a) At 22°. (b) At 84°. (c) At 126°.

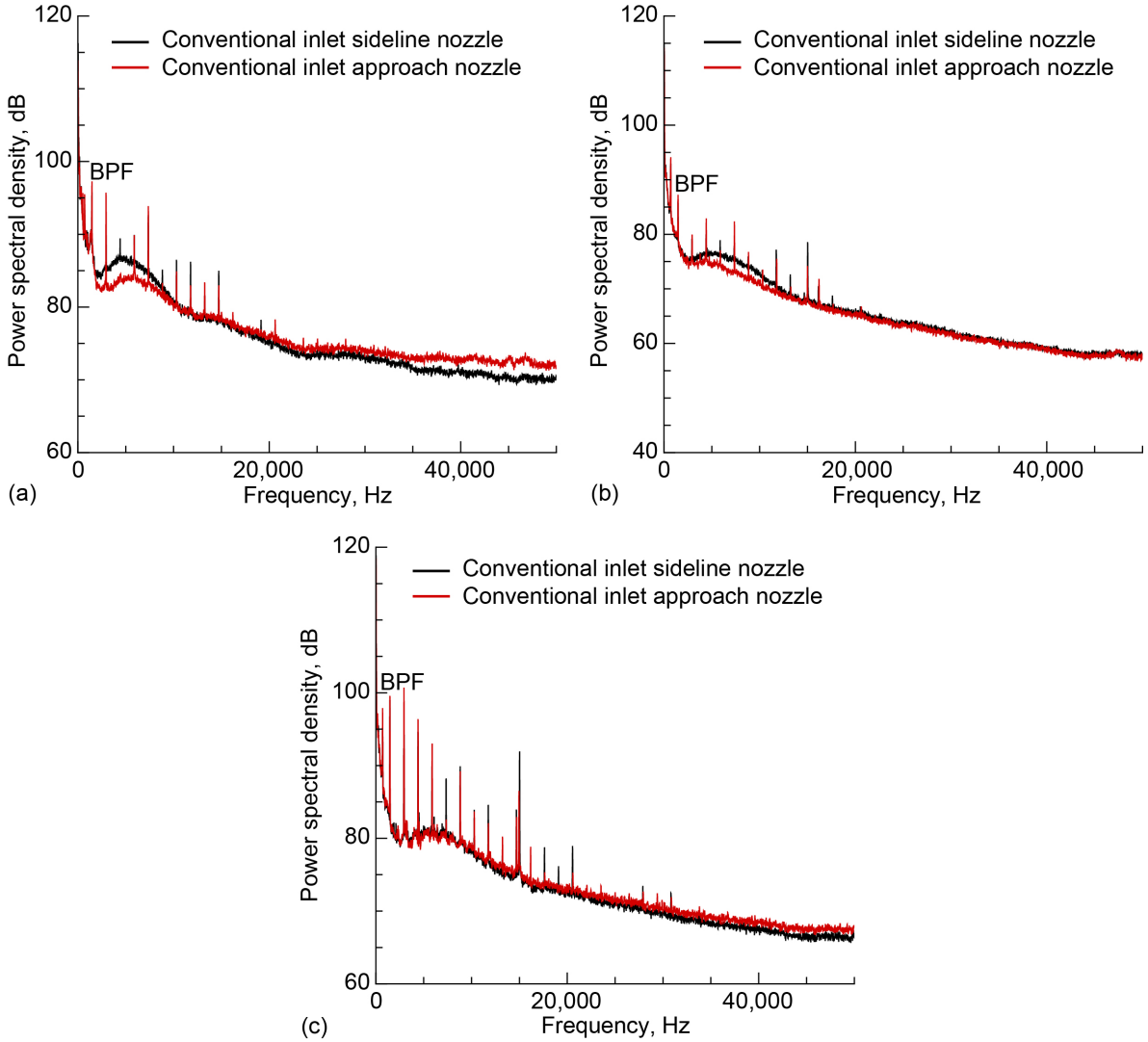

Figure 13.—One-foot lossless spectra for 6,153-rpmc condition, showing sideline and approach nozzle comparisons using conventional inlet. (a) At 22°. (b) At 84°. (c) At 126°.

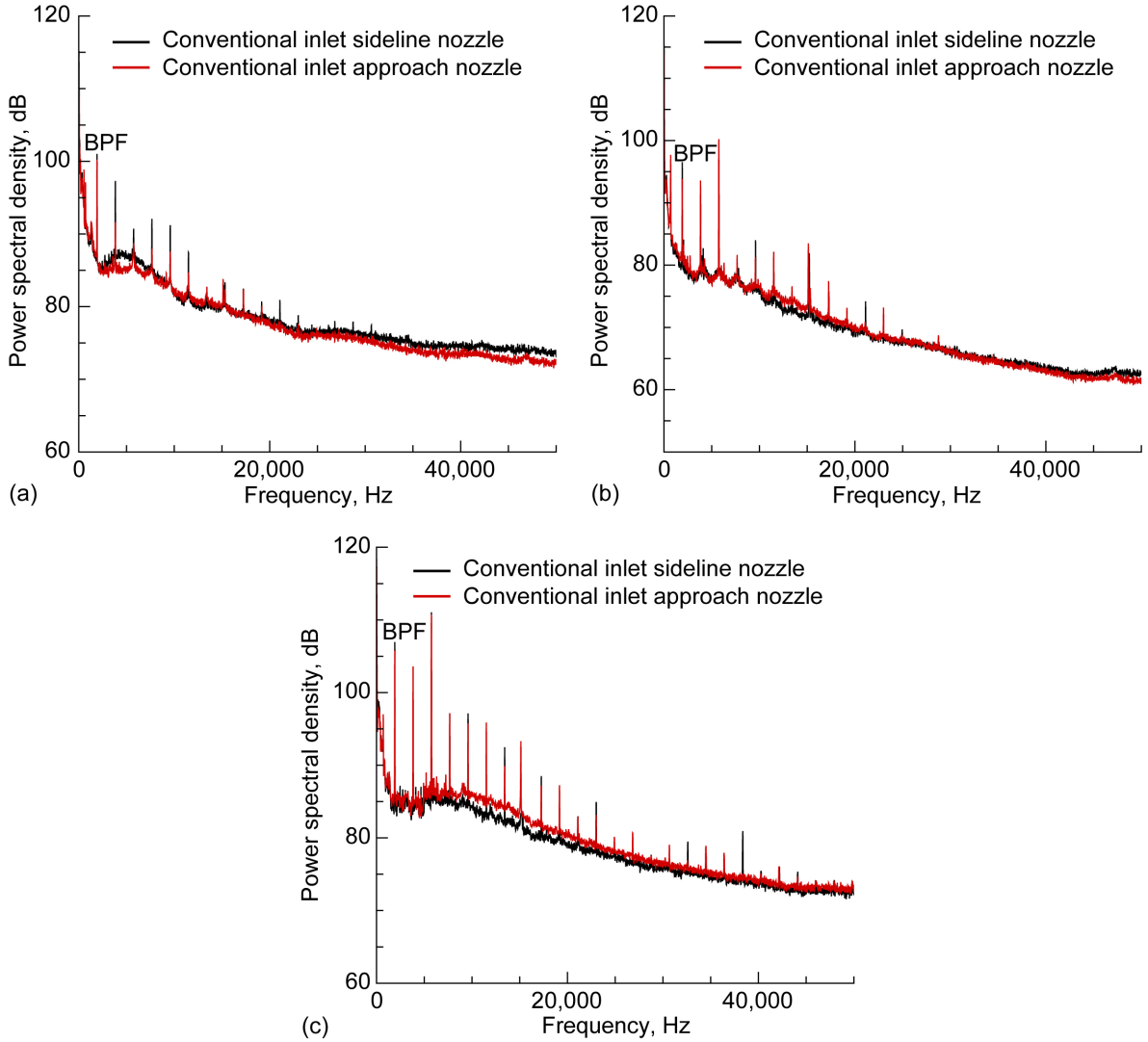

Figure 14.—One-foot lossless spectra for 8,000-rpmc condition, showing sideline and approach nozzle comparisons using conventional inlet. (a) At 22°. (b) At 84°. (c) At 126°.

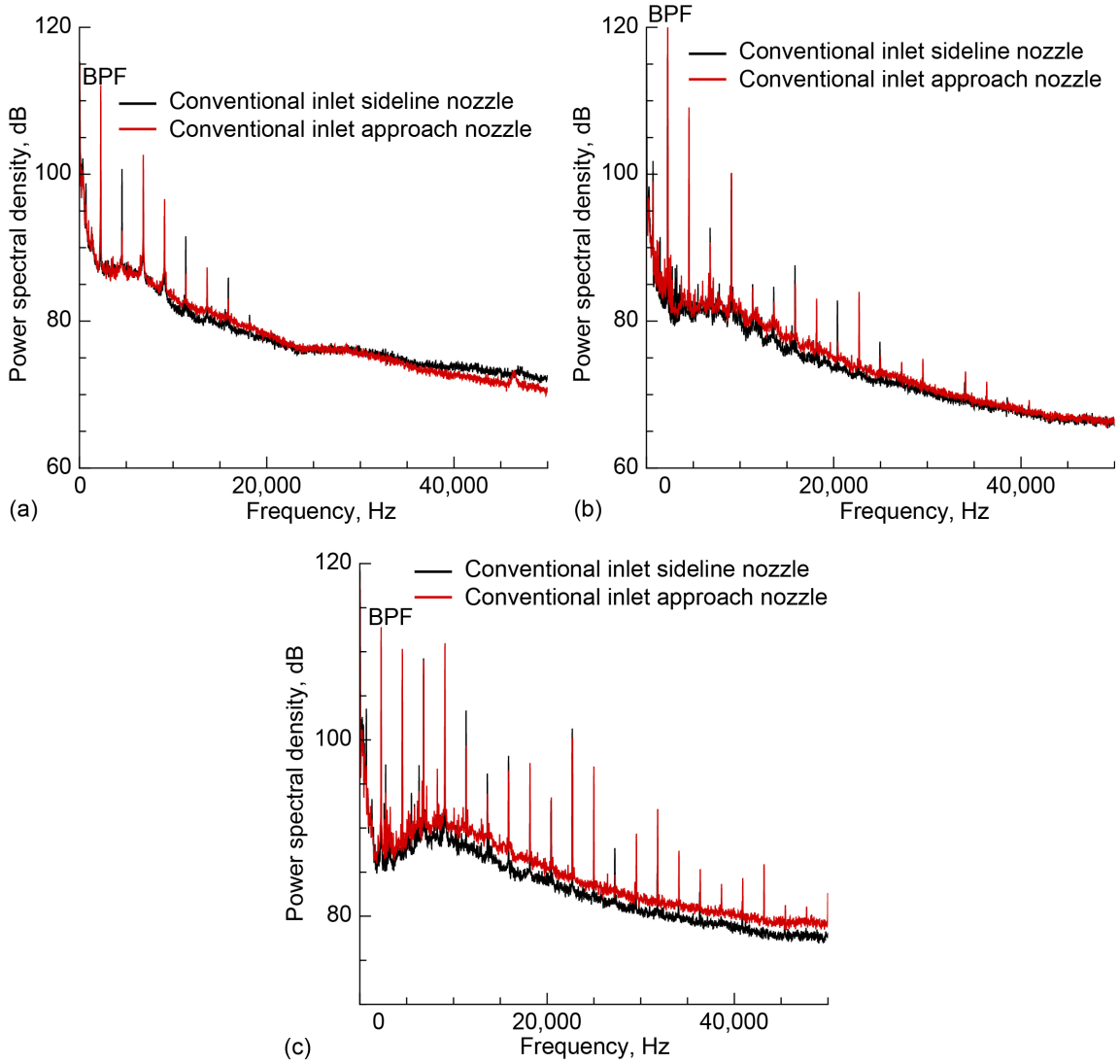

Figure 15.—One-foot lossless spectra for 9,484-rpmc condition, showing sideline and approach nozzle comparisons using conventional inlet. (a) At 22°. (b) At 84°. (c) At 126°.

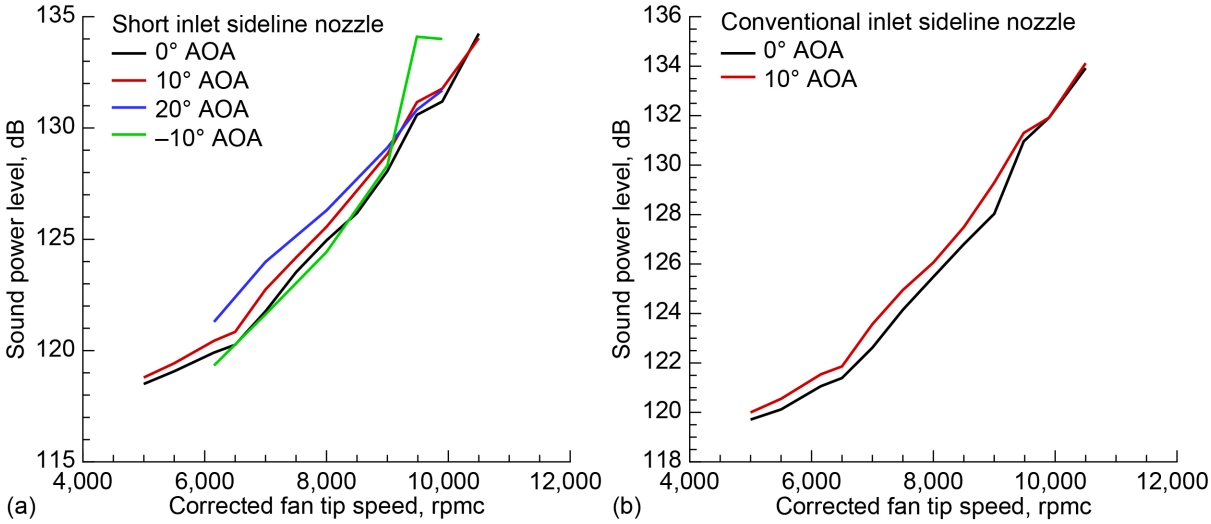

Figure 16.—Overall power levels versus corrected fan tip speed (rpmc), showing sideline nozzle at different AOA. (a) For short inlet. (b) For conventional inlet.

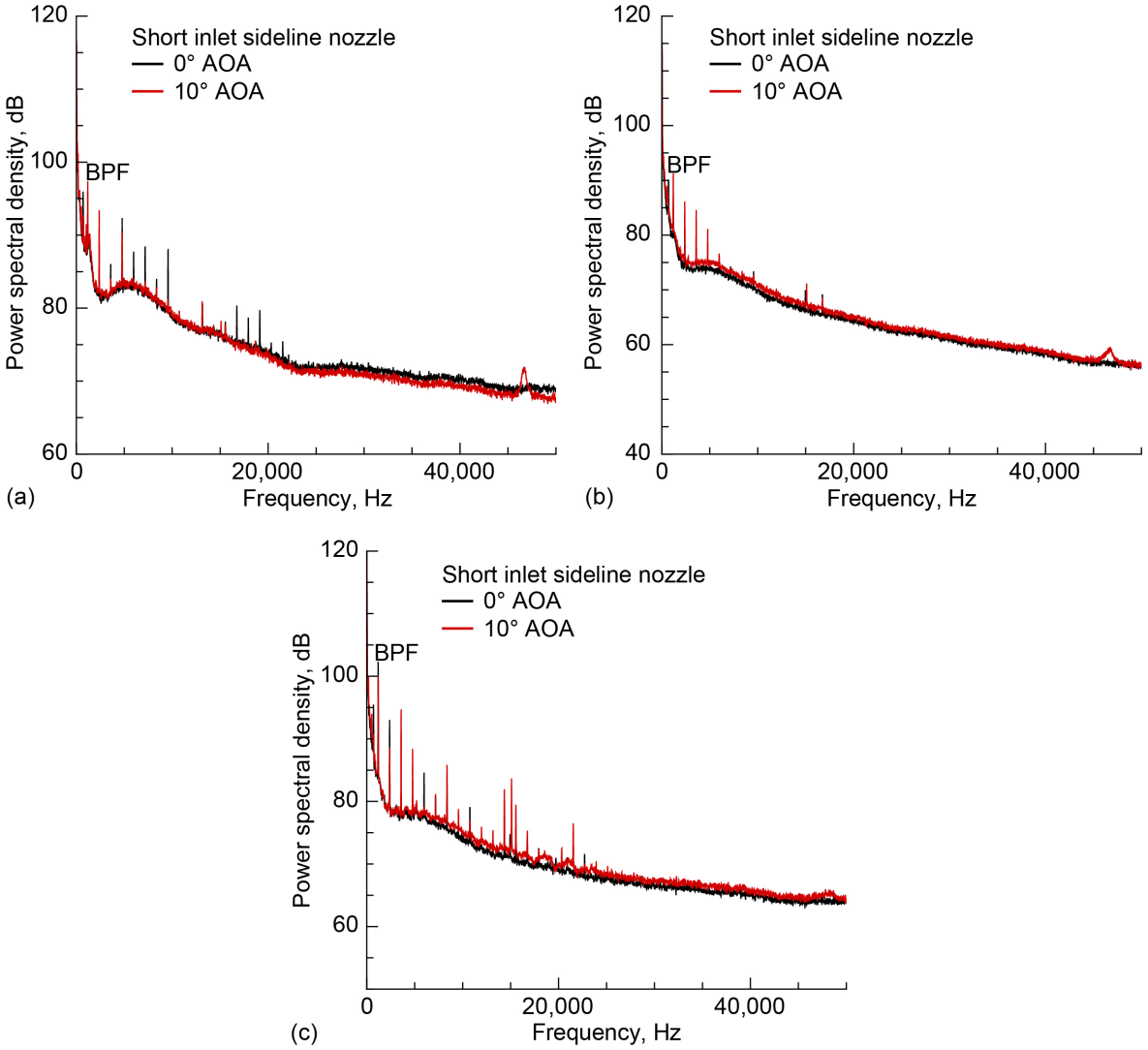

Figure 17.—One-foot lossless spectra for 5,000-rpmc condition, showing short inlet sideline nozzle configuration at 0° and 10° AOA. (a) For 22°. (b) For 84°. (c) For 126°.

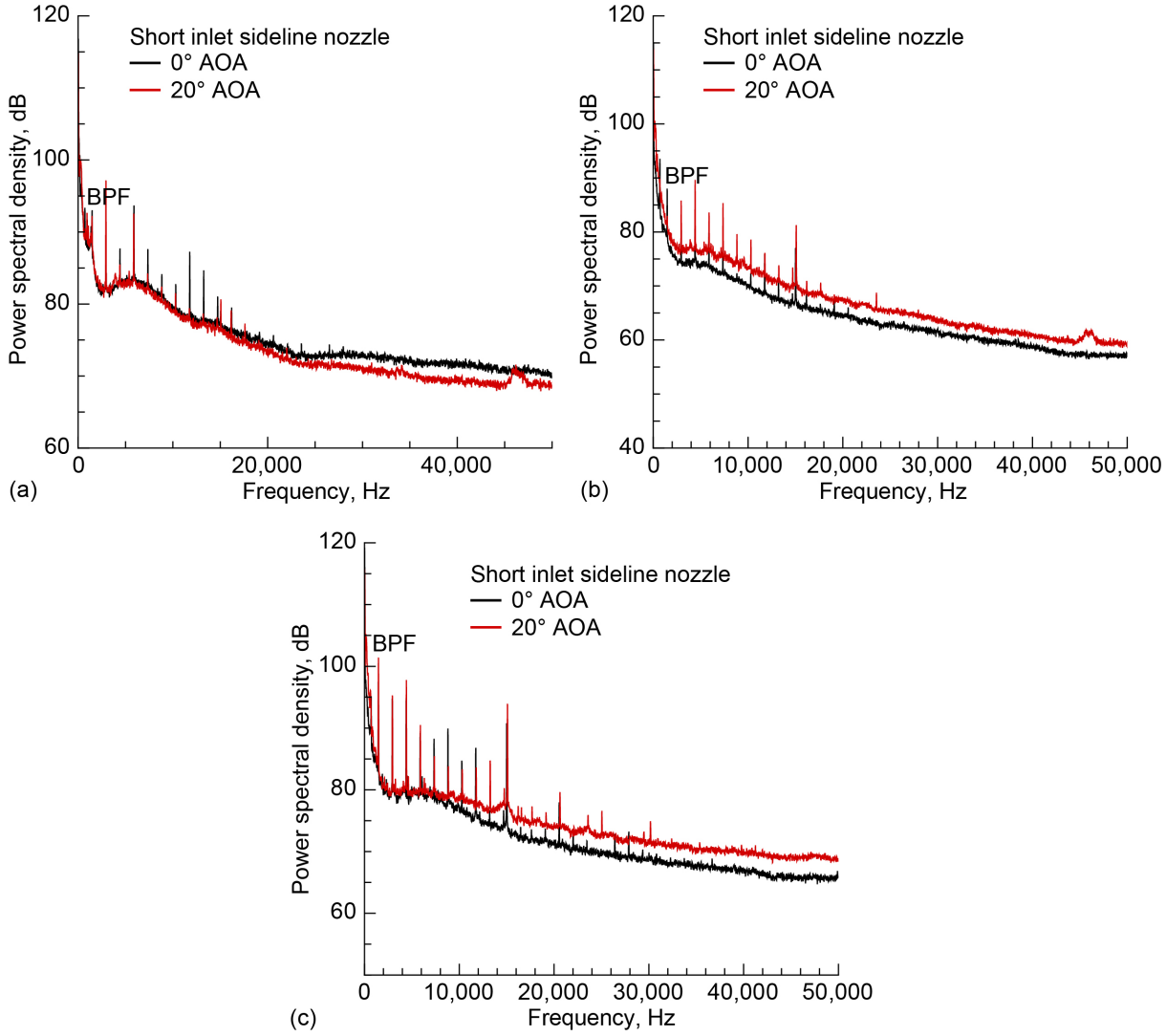

Figure 18.—One-foot lossless spectra for 6,153-rpmc condition showing short inlet sideline nozzle configuration at 0° and 20° AOA. (a) For 22°. (b) For 84°. (c) For 126°.

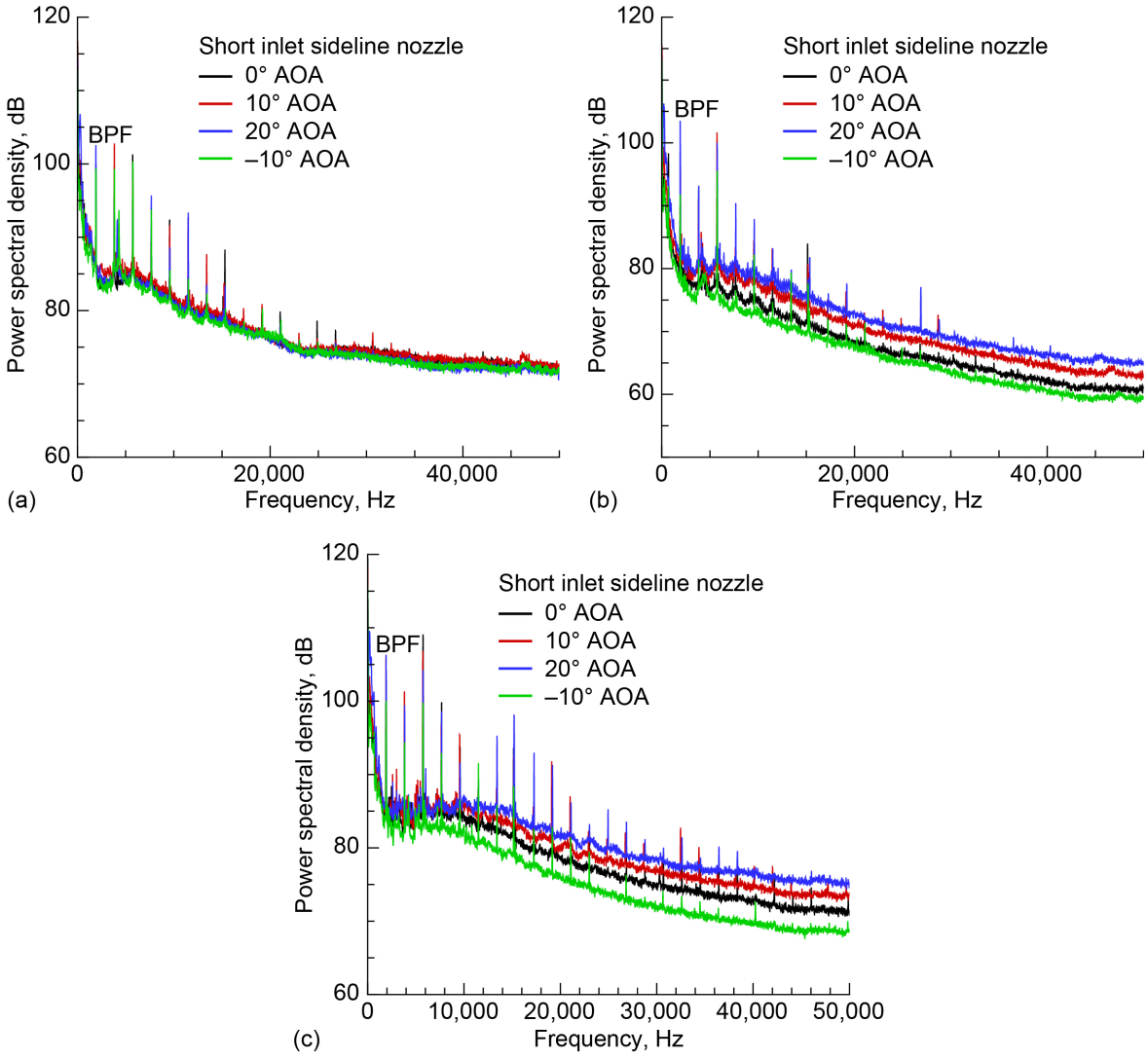

Figure 19.—One-foot lossless spectra for 8,000-rpmc condition, showing short inlet sideline nozzle configuration at 0°, 10°, 20°, and –10° AOA. (a) For 22°. (b) For 84°. (c) For 126°.

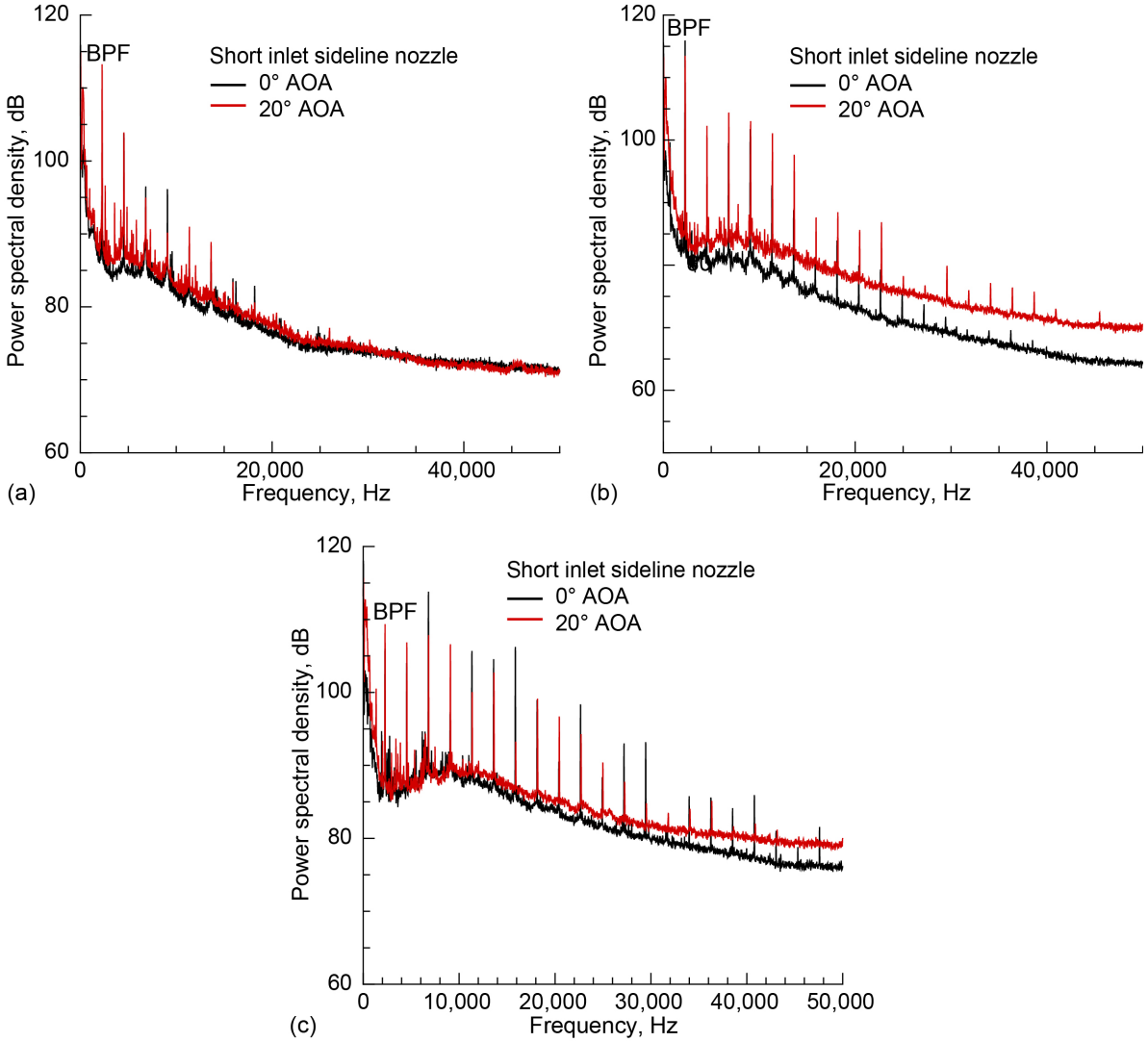

Figure 20.—One-foot lossless spectra for 9,484-rpmc condition, showing short inlet sideline nozzle configuration at 0° and 20° AOA. (a) For 22°. (b) For 84°. (c) For 126°.

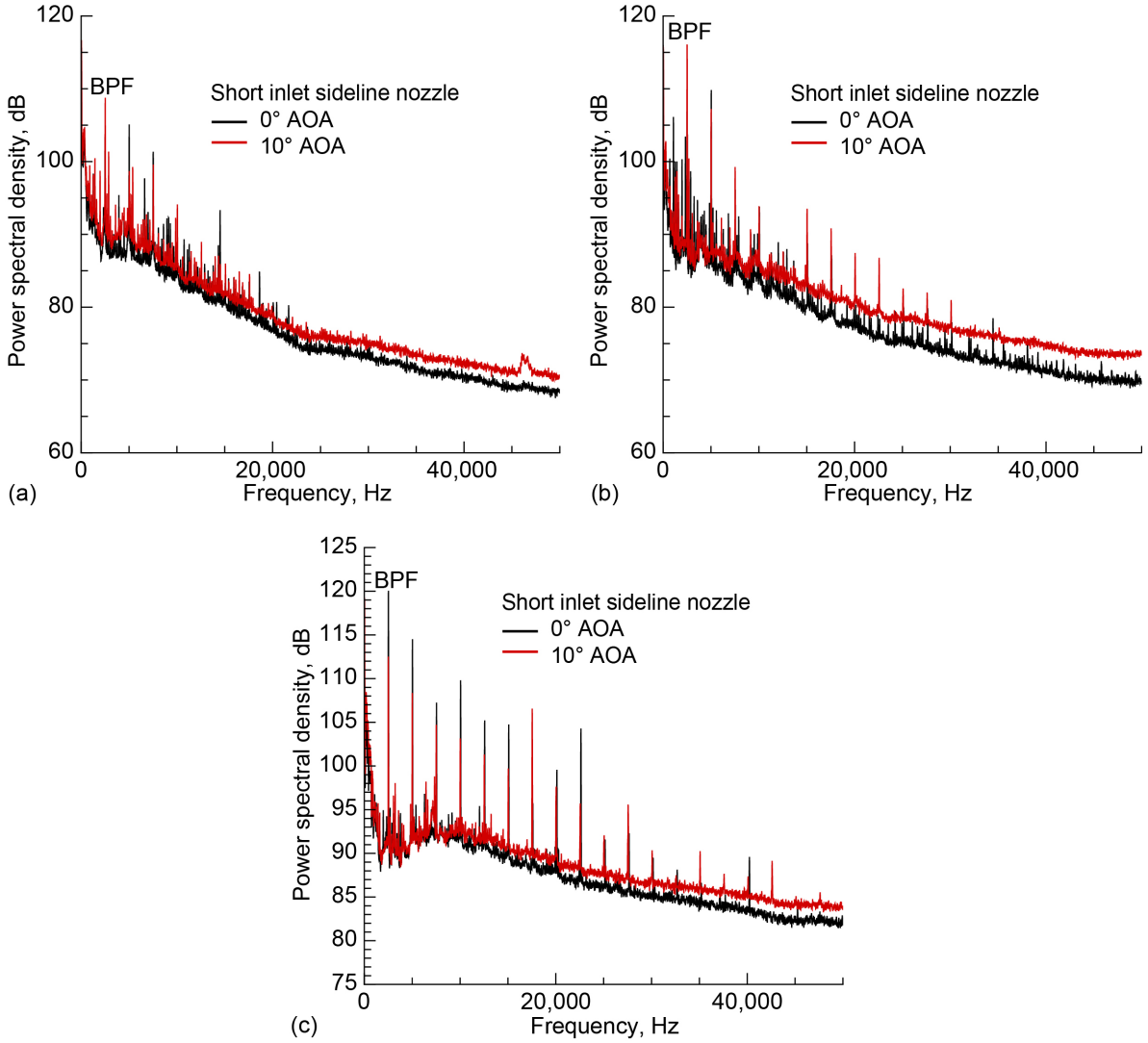

Figure 21.—One-foot lossless spectra for 10,500-rpmc condition, showing short inlet sideline nozzle configuration at 0° and 10° AOA. (a) For 22°. (b) For 84°. (c) For 126°.

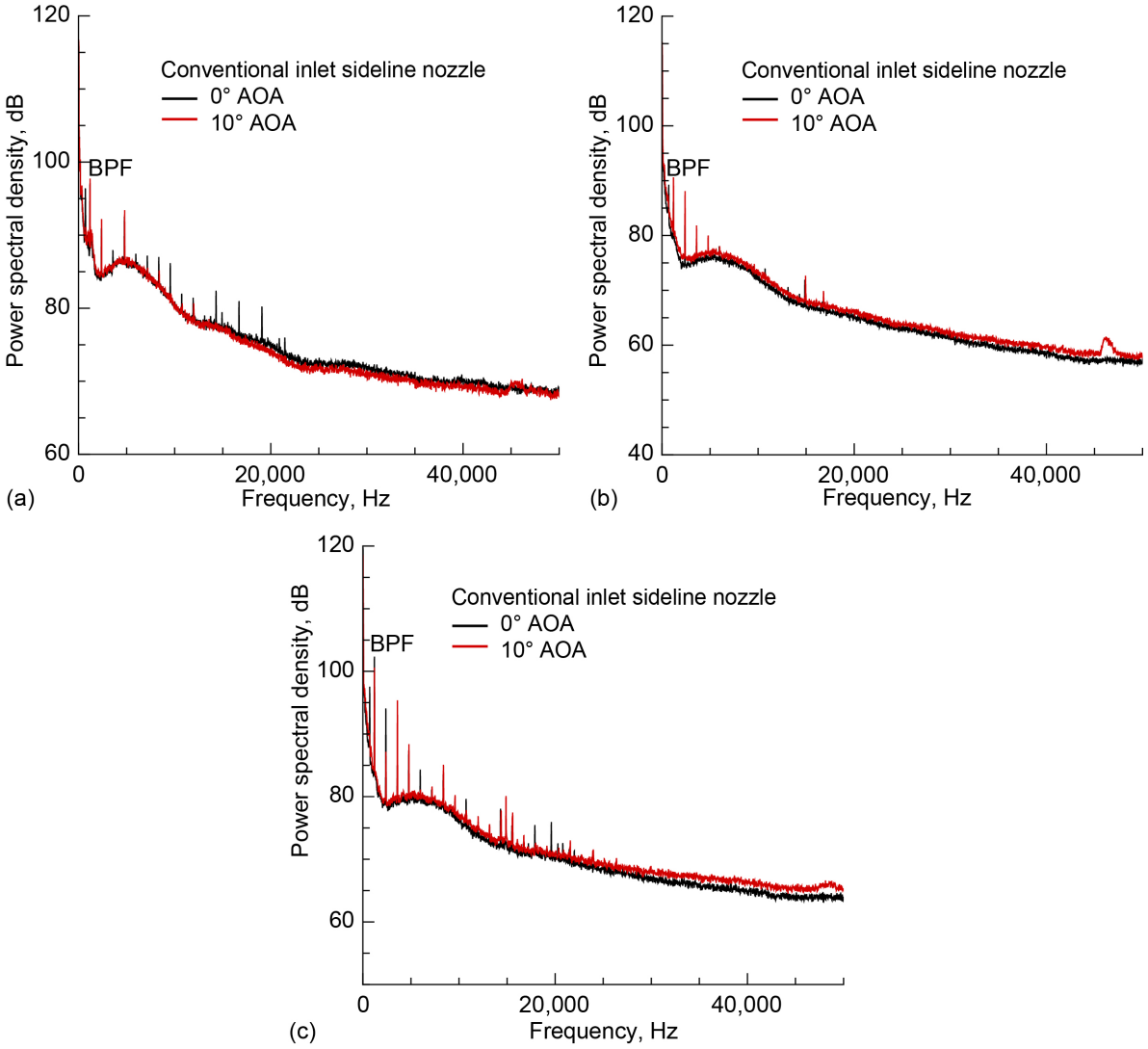

Figure 22.—One-foot lossless spectra for 5,000-rpmc condition, showing conventional inlet sideline nozzle configuration at 0° and 10° AOA. (a) For 22°. (b) For 84°. (c) For 126°.

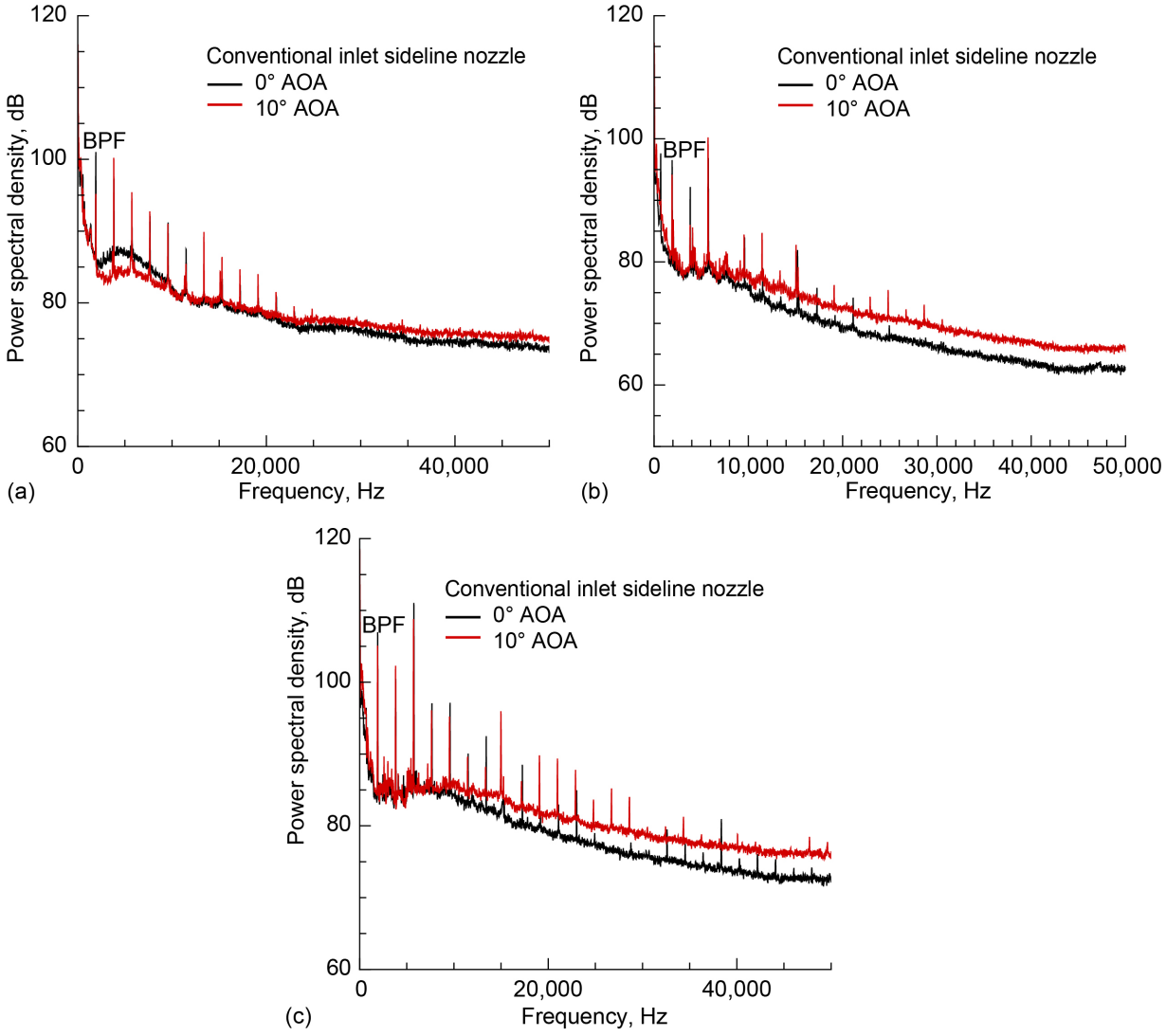

Figure 23.—One-foot lossless spectra for 8,000-rpmc condition, showing conventional inlet sideline nozzle configuration at 0° and 10° AOA. (a) For 22°. (b) For 84°. (c) For 126°.

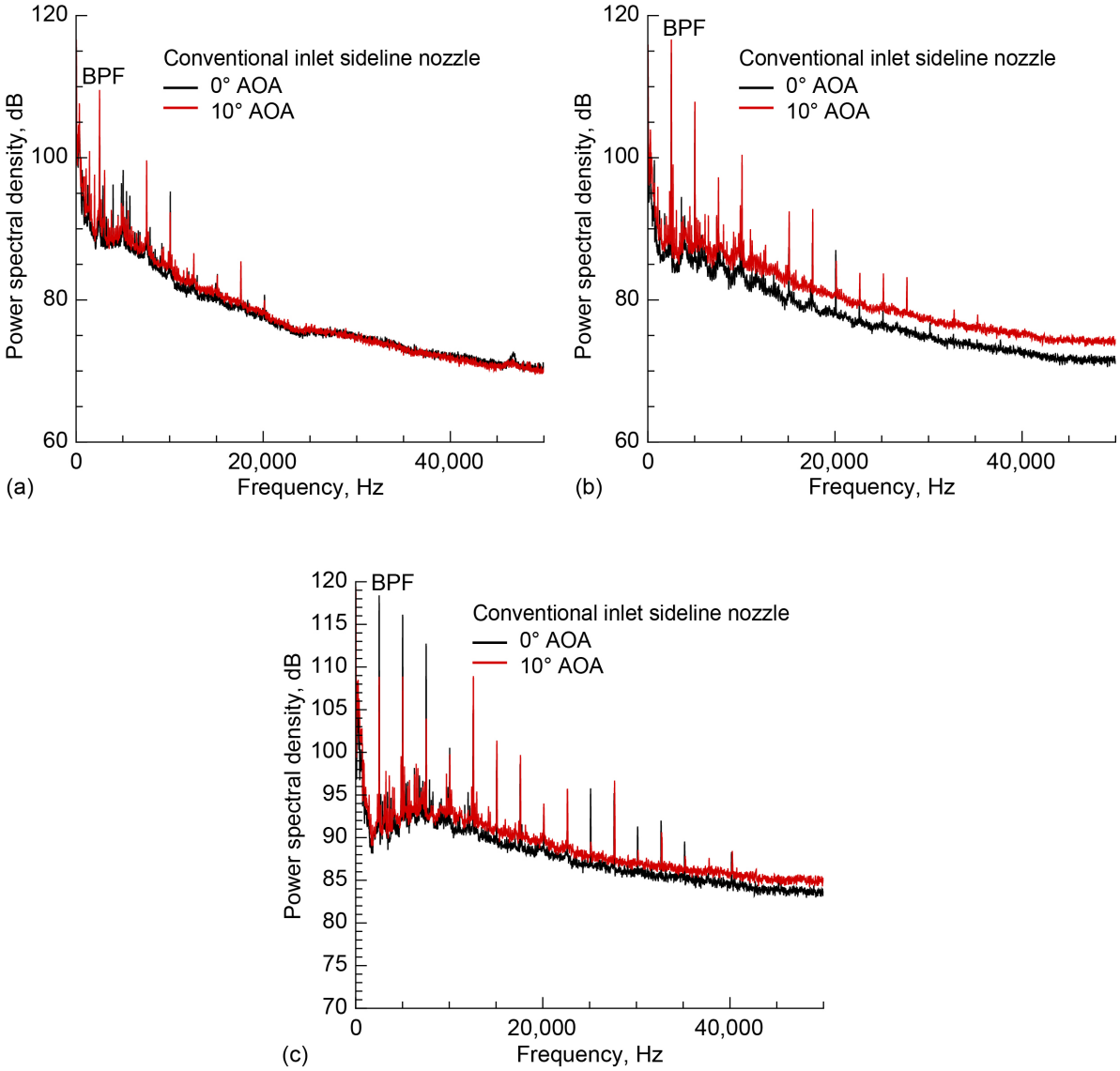

Figure 24.—One-foot lossless spectra for 10,500-rpmc condition, showing conventional inlet sideline nozzle configuration at 0° and 10° AOA. (a) For 22°. (b) For 84°. (c) For 126°.

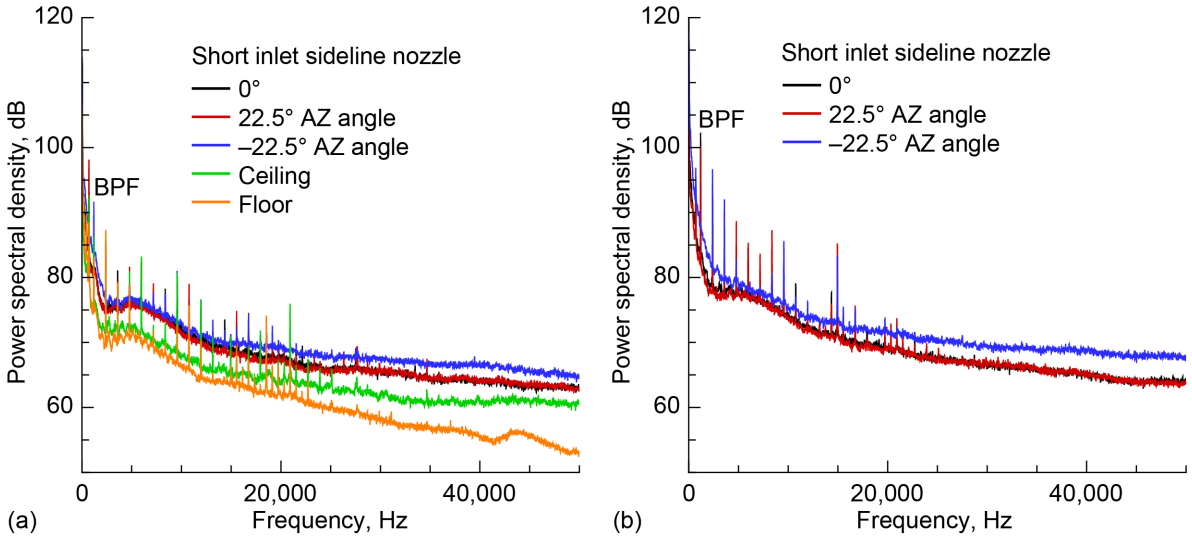

Figure 25.—One-foot lossless spectra for 5,000-rpmc condition, showing short inlet sideline nozzle configuration. (a) Shows 49° emitted angle measurements at five different azimuthal angles. (b) Shows 126° emitted angle measurements for three different azimuthal angles.

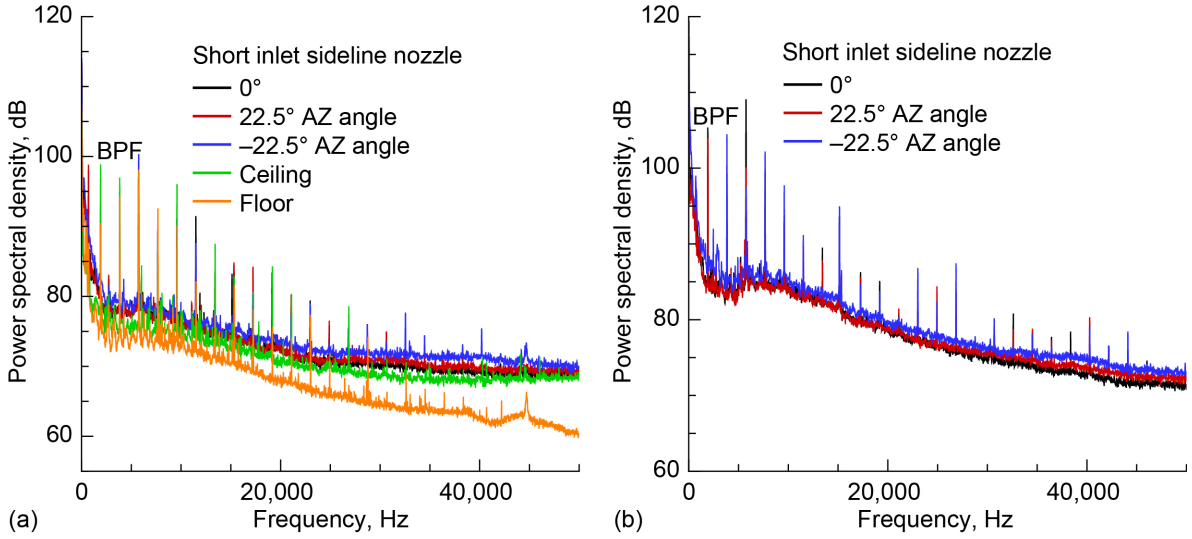

Figure 26.—One-foot lossless spectra for 8,000-rpmc condition, showing Short Inlet Sideline Nozzle configuration. (a) Shows 49° emitted angle measurements at five different azimuthal angles. (b) Shows 126° emitted angle measurements for three different azimuthal angles.

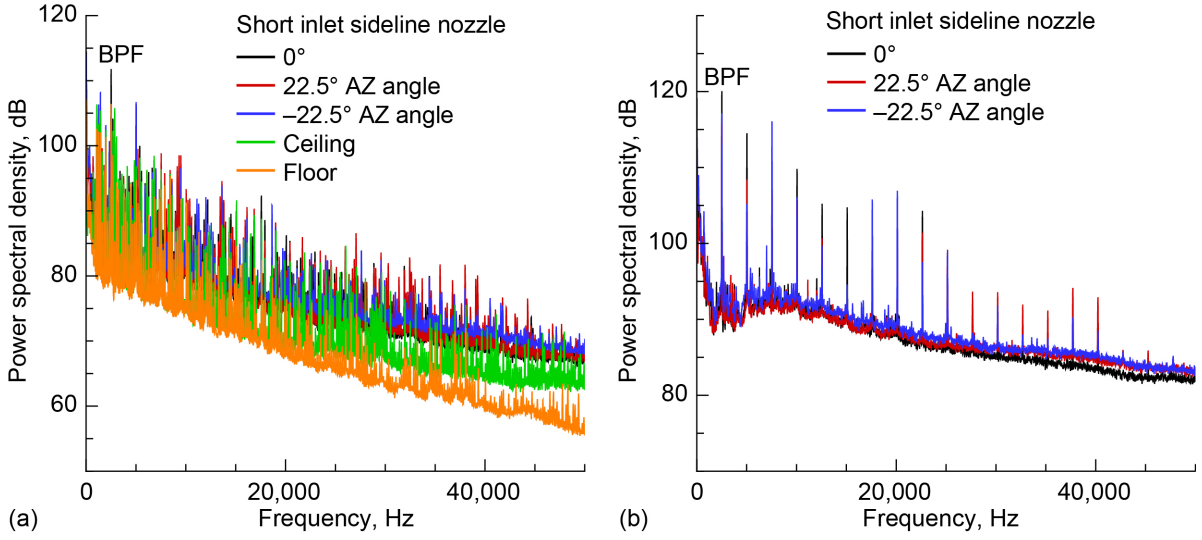

Figure 27.—One-foot lossless spectra for 10,500-rpmc condition, showing short inlet sideline nozzle configuration. (a) Shows 49° emitted angle measurements at five different azimuthal angles. (b) Shows 126° emitted angle measurements for three different azimuthal angles.

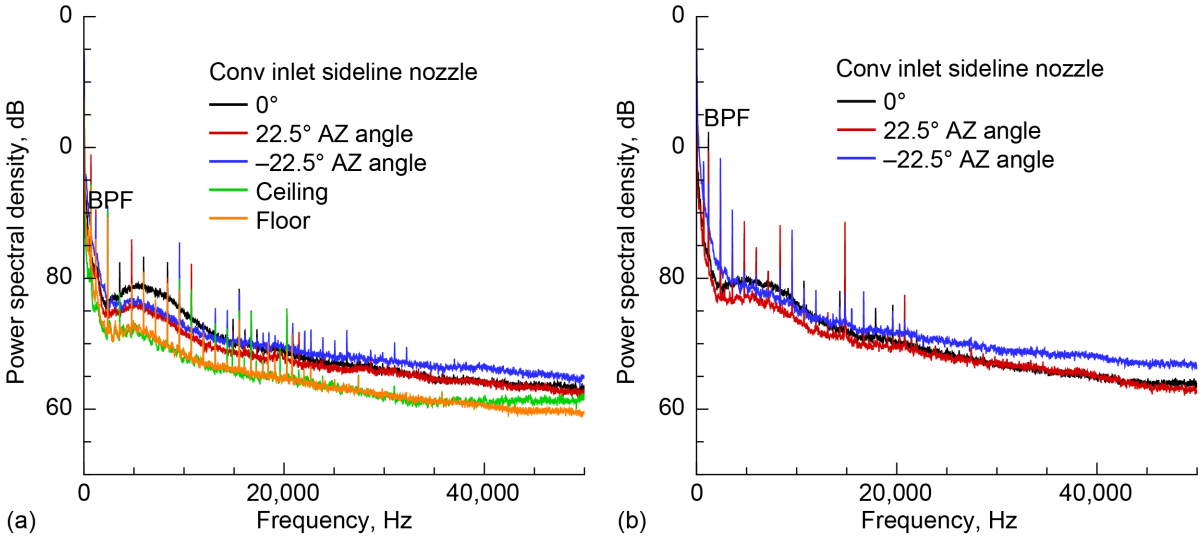

Figure 28.—One-foot lossless spectra for 5,000-rpmc condition, showing conventional inlet sideline nozzle configuration. (a) Shows 49° emitted angle measurements at five different azimuthal angles. (b) Shows 126° emitted angle measurements for three different azimuthal angles.

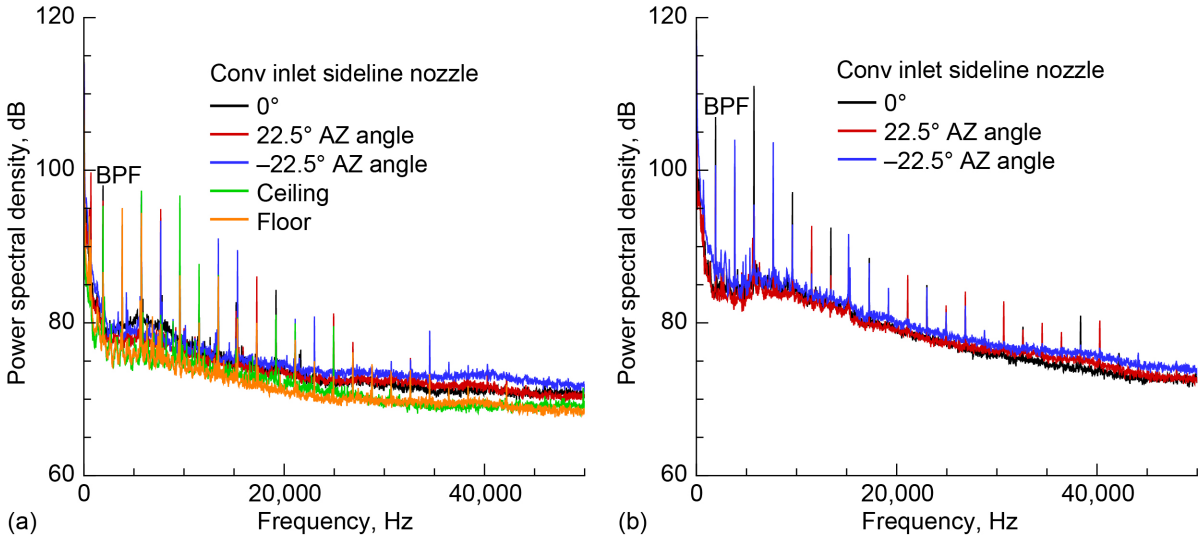

Figure 29.—One-foot lossless spectra for 8,000-rpmc condition showing conventional inlet sideline nozzle configuration. (a) Shows 49° emitted angle measurements at five different azimuthal angles. (b) Shows 126° emitted angle measurements for three different azimuthal angles.

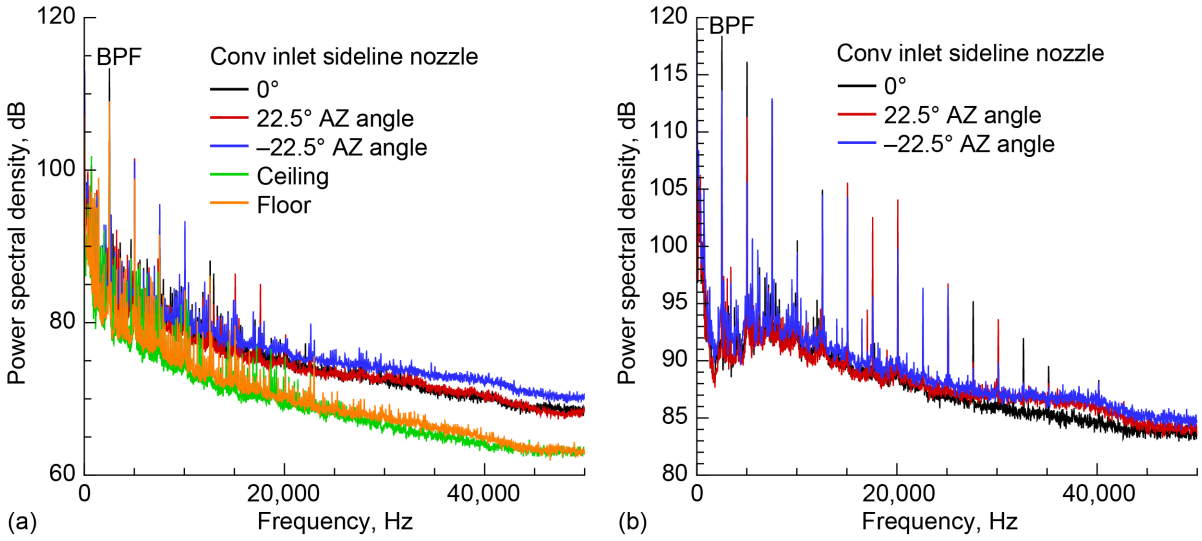

Figure 30.—One-foot lossless spectra for 10,500-rpmc condition, showing conventional inlet sideline nozzle configuration. (a) Shows 49° emitted angle measurements at five different azimuthal angles. (b) Shows 126° emitted angle measurements for three different azimuthal angles.